Southeastern Geology: Volume 44, No. 1
October 2005

Editor in Chief: S. Duncan Heron, Jr.

Abstract

Academic journal published quarterly by the Department of Geology, Duke University.

SOUTHEASTERN GEOLOGY

Vol. 44, No. 1 October 2005

SOUTHEASTERN GEOLOGY

PUBLISHED

at

DUKE UNIVERSITY

Duncan Heron

Editor in Chief

David M. Bush

Editor

This journal publishes the results of original research on all phases of geology, geophysics, geochemistry and environmental geology as related to the Southeast. Send manuscripts to **David Bush, Department of Geosciences, University of West Georgia, Carrollton, Georgia 30118, for Fed-X, etc. 1601 Maple St.,** Phone: 678-839-4057, Fax: 678-839-4071, Email: dbush@westga.edu. Please observe the following:

1) Type the manuscript with double space lines and submit in duplicate, or submit as an Acrobat file attached to an email.
2) Cite references and prepare bibliographic lists in accordance with the method found within the pages of this journal. Data citations examples can be found at http://www.geoinfo.org/TFGeosciData.htm
3) Submit line drawings and complex tables reduced to final publication size (no bigger than 8 x 5 3/8 inches).
4) Make certain that all photographs are sharp, clear, and of good contrast.
5) Stratigraphic terminology should abide by the North American Stratigraphic Code (American Association Petroleum Geologists Bulletin, v. 67, p. 841-875).
6) Email Acrobat (pdf) submissions are encouraged.

Subscriptions to *Southeastern Geology* for volume 44 are: individuals - $24.00 (paid by personal check); corporations and libraries - $35.00; foreign $45. Inquires should be sent to: **SOUTHEASTERN GEOLOGY, DUKE UNIVERSITY, DIVISION OF EARTH & OCEAN SCIENCES, BOX 90233, DURHAM, NORTH CAROLINA 27708-0233**. Make checks payable to: *Southeastern Geology.*

Information about **SOUTHEASTERN GEOLOGY** is on the World Wide Web including a searchable author-title index 1958-2001 (Acrobat format). The URL for the Web site is: http://www.southeasterngeology.org

SOUTHEASTERN GEOLOGY is a peer review journal.

ISSN 0038-3678

SOUTHEASTERN GEOLOGY

Table of Contents

Volume 44, No. 1 October 2005

EDITOR'S PAGE

I welcome David M. Bush as editor of **Southeastern Geology**. David is Professor of Geology in the Department of Geosciences at the University of West Georgia. Please submit manuscripts to him at:

David M. Bush
Department of Geosciences
University of West Georgia
Carrollton GA 30118
dbush@westga.edu
for Fed-X, etc. use 1601 Maple St., Phone 678-839-4057

Of course you can still submit manuscripts to me at the Duke address on the inside cover, but it might speed things up if you submit to David. As always Acrobat submission is encouraged.

Thanks for your support of **Southeastern Geology**.

Duncan Heron
Editor-in-Chief

SOUTHEASTERN GEOLOGY
V. 44, No. 1, October 2005, p. 1-17

FETCH LIMITED BARRIER ISLANDS OF CHESAPEAKE BAY AND DELAWARE BAY

DAVID A. LEWIS[1]

Duke University Nicholas School of Earth and Environmental Sciences
PO Box 90228
Durham, NC 27708
david.lewis@duke.edu

J.A.G. COOPER

University of Ulster Centre for Coastal and Marine Research
Cromore Road
Coleraine, BT52 1SA

ORRIN H. PILKEY

Duke University Nicholas School of Earth and Environmental Sciences
PO Box 90228
Durham, NC 27708

1. Corresponding author.

ABSTRACT

Barrier islands within bays, lagoons, estuaries and other protected waters have never been the subject of systematic research on a large scale. Within both the Chesapeake and Delaware Bays, barrier islands are numerous and widely distributed. Totaling more than 300 in number, these fetch limited barrier islands exhibit a range of morphologies uncommon along open ocean shorelines. We group the barrier islands in the two bays into three primary categories based on their morphology and location. In general, they are much shorter (~1km), narrower (<25m), and lower (1-2m) than their open ocean analogs, yet they behave in much the same way in their response to oceanographic processes. The greatest difference between ocean and bay barriers is the strong control of evolutionary processes by vegetation, usually salt marsh, in the bays.

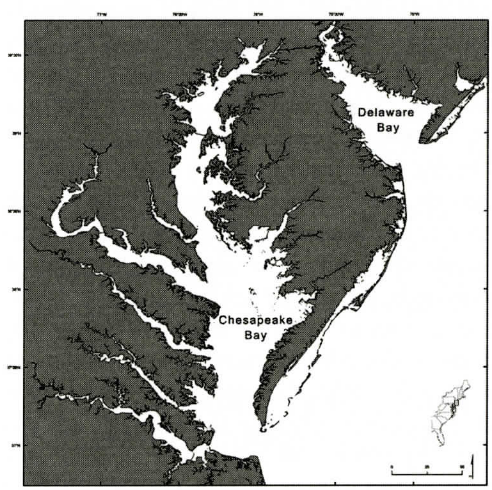

Figure 1: A regional map of the Chesapeake and Delaware Bays.

INTRODUCTION

For decades barrier islands have been the focus of intense scrutiny (for example Hoyt 1967, Schwartz 1973, Glaeser 1978, Hayes 1979, Oertel 1985, McBride *et al* 1995, Martinez *et al* 2000, Stutz 2002). They are numerous and particularly well-studied along North America's Mid-Atlantic coastline (Swift 1975, Davis 1994, Riggs *et al* 1995, Moslow and Heron 1994, Hayes 1994). However, barrier islands *within* bays such as the Chesapeake and Dela-

Figure 2: A typical active fetch limited barrier island, backed by a salt marsh lagoon on the western shore of the Chesapeake Bay.

Figure 3: A patch of junctus grass that completely surrounds an inactive barrier island.

ware (Figure 1) have received little attention and have never explicitly been the subject of any systematic research.

The barriers along the shorelines of both bays are abundant, well-developed, and consistent with the common definition of a barrier island. Oertel (1985) states that a barrier island must be (1) an elongated body of unconsolidated sediment (typically sand) (2) bound by inlets (3) backed by a lagoon (4) fronted by a marine shoreface (5) perched upon a barrier platform and (6) protecting a mainland coastline.

In this paper we distinguish *active* barrier islands (Figure 2), those that form within a fetch limited environment and are subjected to wave and current activity, resulting in modification of the islands, either or both constructive or destructive from *inactive* islands (Figure 3), which are those being currently modified more by subaerial rather than by oceanographic processes (usually because the features are enclosed by salt marsh and mangroves). In this report we focus exclusively on the active barrier islands of the Chesapeake and Delaware Bays.

There are nearly 7500 such *active* barrier island features within lagoons, bays, and other protected marine bodies around the world– a figure nearly three times the number of open ocean barrier islands (Stutz *et al*, 2002). Though abundant and widely distributed, fetch limited barrier islands comprise just one quarter the total shoreline distance covered by open ocean barrier islands, globally. Size is the most glaring difference between barrier islands along open ocean and fetch limited coastlines – fetch limited barrier islands are rarely much more than 1km long, while those on ocean shorelines are usually longer than 10km.

Our global survey and the results of field and remote analysis of barrier islands in the Chesapeake and Delaware Bays focus on low-energy sheltered shorelines which total over 10,000km of estuarine shoreline. Barrier island research more frequently focuses upon the socially and economically more important open ocean coastlines. However, the Chesapeake and Delaware Bays are large wetland ecosystems, and also important for navigation, trade, defense, and recreation. This paper provides an analysis and discussion of the distribution, morphology, and evolution of the bays' barrier island shorelines that have hitherto been overlooked in the literature. Our research relied heavily upon aerial photos, satellite imagery, USGS 1:24,000 topographic maps, NOAA navigational charts, and historical maps and charts. In addition, we conducted field and aerial reconnaissance, plotting the distribution of barrier islands throughout the Chesapeake Bay and the Delaware Bay, and noting trends in island morphology and behavior.

As this research is among the first of its kind to focus on low energy barrier island systems, it is subject to unique limitations. In addition to distinguishing between active and inactive barrier islands, we found it important to note the difference between islands forming under natural processes and those originating from human design, manipulation, or activity. Given the high degree of development and modification throughout both bays, *anthropic* islands are abundant. Differentiating anthropic islands, which are usually formed from dredge spoil, from active islands is the foremost challenge among the factors imposing limits upon this research. The overwhelming dominance of small sand features among the population of barrier islands in the bays, mostly sand bars atop salt marsh rims 10 to 25m in length, posed another concern. Thus, the minimum island length was arbitrarily established as 50m, primarily owing to limitations in remotely collected data and the accuracy of published maps and charts.

SETTING

The Chesapeake and Delaware Bays are located in the Mid-Atlantic Region of the United States. Both bays are large drowned river estuaries, subject to a highly variable temperate climate regime on the tectonically passive Atlantic margin of North America. The Delmarva Peninsula and Cape Charles protect the Chesapeake Bay from ocean swells, while southern New Jersey and Cape May shelter the Delaware Bay. The bays experience freezing during the winter months and regular, modest flooding during the spring. Nordstrom and Sherman (1982) describe the effects of freezing on estuarine beaches at mid-latitudes, including extreme recession of shorelines, ice scour, wave dampening, and melt runoff. Both bays experience their most severe weather in the late autumn and winter, with storms primarily coming from the north and northeast (Hardaway *et al* 2001).

In terms of size, the bays differ by an order of magnitude: Chesapeake Bay is 11600km^2 in area and has nearly ten thousand kilometers of tidally influenced shoreline, whereas the Delaware Bay, which is 2100km^2 in area has just one thousand kilometers of shoreline. The extreme difference in shoreline length is attributable to the more than one dozen tributary estuaries within the Chesapeake Bay. The Delaware Bay has just one main estuary and its shorelines are comparatively straight and smooth. The length of the primary channel of the Chesapeake Bay is 288km, greater than that of the Delaware Bay (84km) by a factor of 3.5. In addition, the Chesapeake Bay shows a high degree of variability in its shoreline orientation and morphology (Rosen 1980). The non-barrier island shoreline of the Chesapeake Bay is either marsh, barrier beach (not island), heavily modified by humans (seawalled, etc.), rocky, muddy, or riparian. The shorelines of Delaware Bay are characteristically straight (homogeneously oriented) and sandy.

Chesapeake Bay is as much as 53m deep, but on average is 8-10m; Delaware Bay is at most 25m deep and on average 10m.

Hobbs (2003) describes the history of Chesapeake Bay. Pre-existing topography – mainly fluvial deposits – strongly influences the shorelines of both bays (Kayan and Kraft 1971). Modern controls on large scale bay evolution include a rising sea level (~2-4mma^{-1}) and drastic human modification of shorelines (seawalling, dredging, dredge spoil disposal, wetland destruction, pollution, and beach nourishment) (Colman and Mixon 1988; Nikitina *et al* 2000; Smith *et al* 2002). Wave heights are typically very low (<0.25m) throughout both bays except during storms; storm surge wave heights can reach anywhere from 2-3m (Hardaway *et al* 2001). Both bays are subject to a diurnal tidal regime with a range of approximately 1m near their openings and less than 0.3m near the head of the bay.

CLASSIFICATION OF FETCH LIMITED BARRIER ISLANDS

In addition to distinguishing between active, inactive, and anthropic islands, we divide active fetch limited barrier islands in Chesapeake and Delaware Bays into three primary categories and two notable sub-categories as shown in Table 1.

Classic fetch limited barrier islands are the most abundant in terms of total length (134km) and are most similar to the Atlantic open ocean coastal plain barrier islands (Figure 4). They are the longest of the three types of islands, averag-

Table 1:

Types of fetch limited barrier islands
I. Active
I.1 Classic
Relict topography
I.2 Marsh fringe
Wraparound
I.3 Two-sided
II. Inactive
III. Anthropic

Figure 4: A classic barrier island on the western margin of the lower Chesapeake Bay. Such islands are very similar in evolutionary processes to open ocean barrier islands. Note that this island is heavily developed.

ing 2.4km, and the widest by a factor of five (Table 2). Most are greater than 100m wide, and some are as much as a kilometer wide. In their morphology and evolution, we determine that classic barrier island behavior is very similar to that of open ocean barriers. Classic islands are prone to extensive overwash and cross-shore migration as well as alongshore elongation forming recurved spits with dynamic inlets. These islands are occasionally lightly developed with homes and fishing shacks.

Marsh fringe barrier islands are the most abundant in number, with 254 islands accounting for nearly 80% of all barrier islands in the two bays. These islands are thin (1-2m) veneers of sediment perched over salt marsh vegetation, peat, or mud (Figure 5). They are often just tens of meters wide and rarely more than a kilometer long (0.5km on average). Many exhibit a crescent shape, concave to the water and trapped between marsh grass outcroppings (Figure 6), vaguely reminiscent of a pocket beach on a lithified coast. The marsh outcrops act as anchor points or headlands that control the development of the barrier island plan form.

Two-sided barrier islands are similar to classic islands in many ways except that they are often subject to significant fetch in multiple directions. They thus develop active barrier beaches on both the lagoon and seaward sides of the island (Figure 7). Indeed, distinguishing the lagoon side from the 'open water' side is quite impossible. Just thirteen of these islands exist in the Chesapeake Bay (none in the Delaware Bay) averaging in length 1km apiece. Historic Tangier Island is perhaps the most noteworthy example.

The two interesting sub-classes of islands that we identify in this study are ***wrap around*** and ***relict topography*** islands. Wraparound barrier islands are horseshoe-shaped marsh fringe islands which partially or fully enclose a shal-

Table 2: Summary of island types in the Chesapeake Bay and Delaware Bay

Island Type	Description	Number	Total Length (km)	Avg. Length (km)	Avg. Width (m)
Classic	Long, wider, and straight; most similar to coastal plain barrier islands along ocean coasts	55	134.1	2.4	200
Two-sided	Subject to >10km fetch in two directions; develop barrier beaches on two sides	13	12.1	0.9	65
Marsh Fringe	Short and narrow, with irregular shoreline shape; heavily influenced by marsh grasses	254	118.9	0.5	15
Total		322	265.1	0.8	65

Figure 5: A marsh fringe barrier island on the eastern shore of the Delaware Bay.

Figure 6: Two marsh fringe barrier islands between marsh mud capes; these islands are similar in origin to pocket beaches on rocky coasts.

Figure 7: The southern tip of Tangier Island in Chesapeake Bay, shown here, is a two-sided island. Fetch is essentially the same on both sides of the island, so the distinction between open water and lagoon is meaningless.

Figure 8: A wraparound barrier island on the eastern shore of Chesapeake Bay. The island consists of a series of small strips of sand that enclose a salt marsh.

low marsh lagoon. These islands are influenced by wave attack from a dominant direction, but, through wave refraction around a fixed point (often a marsh remnant), tend to envelop the marsh or open water behind that obstacle (Figure 8). Islands that form from drowned Pleistocene or early Holocene river valley topography or Pleistocene barrier islands are termed relict topography barrier islands. These are a special case of classic type islands, and are often much wider than other classic islands (Figure 9). There are several inactive barrier islands in Chesapeake Bay that appear to have developed on the rims of Carolina bays.

ISLAND MORPHOLOGY AND CHARACTERISTICS

The shape of the fetch limited barrier islands – especially among the marsh fringe islands – varies greatly throughout the Chesapeake Bay, whereas barrier islands in the Delaware Bay are characteristically straight and narrow. In both bays the classic islands are consistently long and narrow (though those influenced heavily by relict topography may be up to 1km wide). Most exhibit minimal or no dune development, although the southernmost islands along the western shore of the Delaware Bay have artifi-

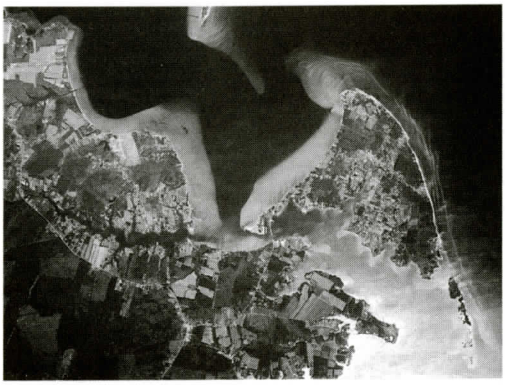

Figure 9: An unusual classic type barrier island formed from relict topography (Photo courtesy of the National Oceanic and Atmospheric Association).

Figure 10: A marsh fringe barrier island on the eastern shore of Delaware Bay, with an extensive dissected marsh mud flat facing the open bay.

Figure 11: A close-up of a marsh flat on the open bay beach with numerous stumps that have been overrun by the migrating barrier island, eastern shore of the Chesapeake Bay.

Figure 12: A classic type fetch limited barrier island on the western shore of Chesapeake Bay with an open water. More commonly, fetch limited barriers in these bays are backed by salt marsh lagoons.

cial dunes protecting houses in some areas. Marsh fringe islands in the Chesapeake Bay adopt a surprising array of irregular, undulating plan forms. At one endpoint, wraparound barriers are highly angular, subject to 20km or more fetch in multiple directions, and enclose a shallow marsh lagoon. At the other extreme, short (~100m) barriers adopt a crescent morphology trapped between marsh grass outcroppings. Two-sided islands are linear with a wave-worked subaerial beach on two sides of the inner upland separated by a narrow cat's eye pond or marsh lagoon.

Although there is considerable variation between classic and marsh fringe islands, the low-tide subaerial portion of most islands extends less than 50m in the cross shore direction. Islands are occasionally as little as 5m across in areas of frequent breaching. These barrier islands are generally thin veneers of sand; trenches revealed that the sand is rarely more than 1-2m thick, though classic islands are occasionally much thicker. The sediment is composed largely of brown, coarse, quartz sand with some gravel. Thin layers of dark 'heavy mineral' deposits are observed on southern barriers, where the marine contribution to the sediment is highest. In the northern parts of both bays, much of the barrier island sediment is terrigenous weathered coastal plain and piedmont sand (Langland

Figure 13: A small gap or 'inlet' between two marsh fringe barrier islands on the western shore of Delaware Bay.

Figure 14: A small ebb tidal delta at the mouth of a man-made channel, separating two marsh fringe islands on the western shore of Delaware Bay. Flood tidal deltas are almost non-existent in the lagoons of the barrier islands of these bays.

Figure 15: Large rhythmic bars in front of two marsh fringe barrier islands in western Chesapeake Bay. These bars are an important sediment sink for this system.

Figure 16: A marsh fringe barrier island in Delaware Bay with an extensive eroded marsh platform.

and Cronin 2003). Discharge from the many rivers entering these two bays has been limited to fine silts and clays in suspended sediment in recent times (Knebel 1989).

In general, barrier islands throughout the bay are located along or near extensive communities of standing salt marsh. Living salt marsh grass (*Spartina alterniflora*) and marsh mud are common features on many beaches (Figure 10). The nearly universal presence of marsh vegetation in such circumstances is interpreted as indication that the island has migrated landward over or onto the marsh and that vegetation is recolonizing in the mud. Frequently stumps are found within salt marsh flats on the beach (Figure 11). In one case a log road from colonial times was observed on a beach marsh flat. That an open water lagoon backs just 21% (71) of the islands (Figure 12) – the balance have standing salt marsh in their backbarrier lagoon – is the best evidence of landward island migration.

Morphologic evolution and transport of sediment in the alongshore direction is clearly evident on classic type islands influenced by high angle storm waves. Many of these exhibit signs of spit elongation and recurving. Comparison of

Table 3: Summary of island chains in the Chesapeake Bay and Delaware Bay

	Chain	Number	Total Length (km)	Avg. Length (km)	Avg. Width (m)	Avg. Lagoon Width (km)	Avg. Fetch (km)
A	Eastern Shore	63	31.7	0.5	20	2.3	23.6
B	Pocomoke Sound	6	0.4	0.1	10	2.8	20.0
C	Tangier Sound (S)	22	17.7	0.8	10	1.7	13.5
D	Tangier Sound (N)	21	7.7	0.4	10	2.4	8.6
E	Deal Islands	5	13.5	2.7	1000	N/A	9.0
F	Nanticoke River	3	2.2	0.7	15	1.2	6.7
G	Hoopers Island	5	1.8	0.4	10	0.4	15.0
H	Bloodsworth Island	5	2.1	0.4	10	N/A	20.0
I	Tangier Islands	29	17.3	0.6	15	N/A	21.7
J	Balls Neck	8	3.2	0.4	10	0.2	33.8
K	Fleet Island	5	8.5	1.7	150	0.3	10.0
L	Gwynn Island	10	18.1	1.8	40	1.2	26.0
M	Plum Tree Island	18	13.2	0.7	45	1.5	24.7
N	Currioman Bay	3	3.5	1.2	25	0.9	10.0
-	No Chain	15	12.3	0.8	290	1.1	11.7
	Chesapeake Bay	218	153.1	0.7	65	1.4	19.2
	Delaware (Eastern)	43	71.4	1.7	45	0.4	15.4
	South Jersey (Western)	28	20.0	0.7	20	1.4	17.4
	Jersey (Western)	34	19.9	0.6	10	1.1	9.5
	Delaware Bay	105	112.0	1.0	30	0.9	16.4
	Total	323	264.3	0.8	50	1.2	17.5

historic maps and charts reveals that marsh fringe islands also migrate and disappear – likely in conjunction with large, singular storms.

True inlets separate less than half of all the islands; most of those with inlets are classic islands. Marsh fringe islands are commonly interrupted only by gaps in the sand deposits. These gaps are usually occupied by mud and marsh grass (Figure 13). Deltas are commonly associated with inlets between classic islands (Figure 14), although most are ebb deltas and flood deltas are extremely rare. Among the classic islands of both bays, tidal deltas appear to be important components of the barrier complex, actively involved in the alongshore movement of sediment from island to island.

Large rhythmic offshore bars are present in both bays, indicating an important nearshore sediment storage system or sink (Figure 15). A true shoreface was rarely observed for marsh fringe islands; instead a broad, eroded marsh platform extends seaward (Figure 16) from the beach. For classic and two-sided islands, a gently sloping sand cover (soft bottom) usually gives way to a peat-mud platform, hardbottom, or the aforementioned ripples within just a few tens of meters from shore.

Chesapeake Bay

We identify 220 active fetch limited barrier islands within the Chesapeake Bay (Figure 17, Table 3). These islands total just 153km in length but comprise large sections of shoreline along the main channel south of the Potomac River. Less than one dozen islands exist along the shorelines of the bay's sub-estuaries (e.g. James River, York River, Potomac River, etc.).

Aside from Fisherman's Island (which we do not consider to be fetch limited), there are no islands in the entrance of the Chesapeake Bay in the vicinity of Hampton Roads and Norfolk. Moreover, for the southern 40km of the eastern (Cape Charles) shoreline, there are no barrier is-

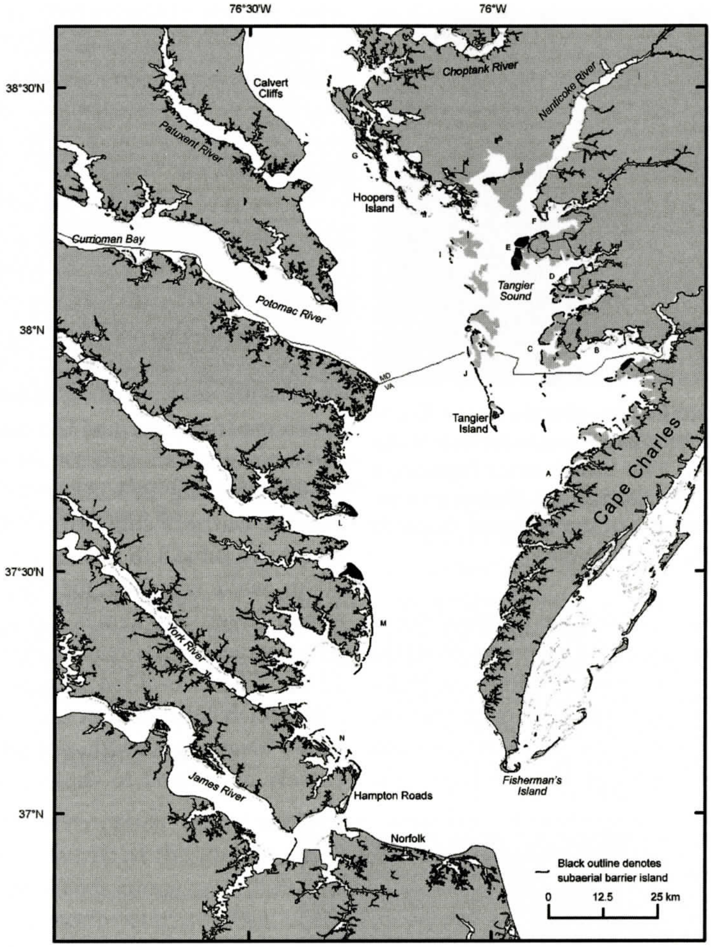

Figure 17: A map showing the location of barrier islands in Chesapeake Bay. The islands are shown by dark lines.

lands at all. As is also observed on southern Cape May, large (10-15m) dunes covered in trees and shrub back the mainland-attached barrier beaches of southern Cape Charles.

The long, southernmost chains of islands on both the eastern and western shores of Chesapeake Bay contain a discontinuous, irregular mix of classic and marsh fringe type islands. The chains are regularly broken by wide inlets corresponding with the outlet points of rivers, both large and small. The islands on the western shore are typically longer (1km) and wider (75m) than those on the eastern shore (0.5km and 20m, respectively). There is also considerable difference in the width of the backbarrier lagoon between the southern islands of the western and eastern shorelines. Barrier islands on the western shore are backed by a lagoon just half the width on average of that on the eastern shore. This difference is likely attributable to the asymmetric distribution of large storms. Nor'easters, the storms that generate the greatest sediment supply originate from the east and tend to push sediment westward.

Islands in the Tangier Sound and near the mouth of the Nanticoke River on the eastern shore are almost exclusively marsh fringe barrier islands and are associated with marsh wetlands as much as 5km wide. The northernmost islands (Hoopers Islands) are short marsh fring-

Figure 18: Classic barrier islands in the Currioman Bay of the Potomac River, a branch of the Chesapeake Bay. The backbarrier lagoon is 300m wide and the islands are densely vegetated. (Photo courtesy of the National Oceanic and Atmospheric Administration)

ing barriers associated with the drowned mainland topographic fragments extending from the mainland. The barrier islands within the Potomac River sub-estuary (to the north) and the James River sub-estuary (to the south) are a mix of classic and marsh fringe barrier islands. The three islands of Currioman Bay (Figure 18), within the Potomac River, are densely vegetated and protect a 300m-wide open water backbarrier lagoon. Excepting their short length, they are indistinguishable from open ocean barrier islands.

Two sets of two-sided islands with their long axes oriented north and south divide the Tangier Sound from the main channel of the Chesapeake Bay. Although they appear to be situated in the geographic center of the bay, they sit on a narrow, submerged shallow topographic high that extends south from the mainland 'neck' between the Nanticoke and Choptank Rivers.

The average shore normal fetch varies considerably among the barrier islands in the Chesapeake. Barriers south of the Potomac River mouth are subject to fetches ranging from 20 to 30km, while islands in the Tangier Sound, Potomac River, and James River are subject to shore perpendicular fetch distances of less than 15km. The two-sided islands are subject to 20km fetch both due east and due west. Neither island length, nor width, nor type appear to be closely correlated to shore normal fetch, al-

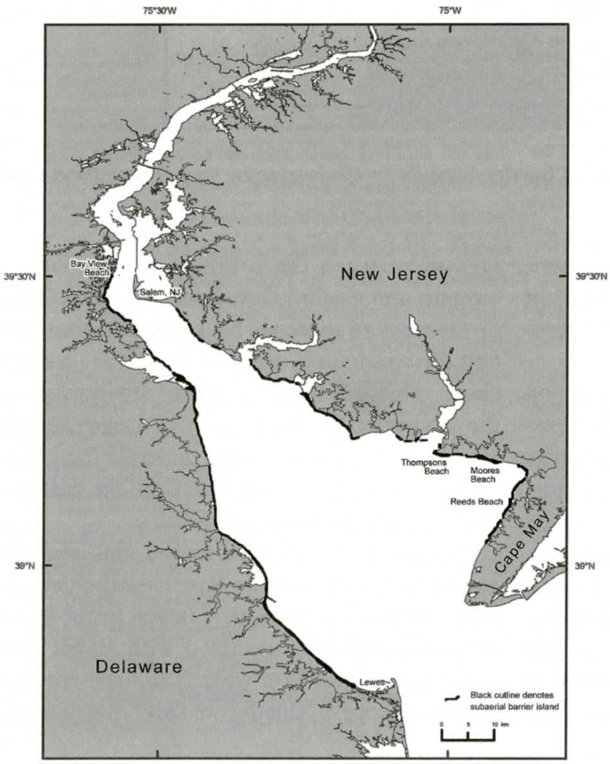

Figure 19: A map showing the location of barrier islands in Delaware Bay. The islands are shown by dark lines.

Figure 20: A portion of a classic barrier island in western Delaware Bay. The classic barrier islands along the lower shorelines are the best developed within Delaware Bay.

though all of the longest islands (>1.5km) are along the main channel of the lower bay where the maximum fetch along the north-south axis of the bay exceeds 50km.

Delaware Bay

There are 105 active fetch limited barrier islands along the shores of the Delaware Bay (Figure 19). The islands comprise 112km of the nearly 1000km of north-south trending, tidally-influenced, estuarine shoreline that stretches to above the city of Philadelphia, PA. Islands are more numerous on the eastern (New Jersey) shoreline, but account for just one-third of the total barrier island shoreline length within this bay. Barrier island development is far more continuous along the western (Delaware) shoreline than along the eastern. Barrier islands run nearly uninterrupted from just north of Lewes, Delaware to Bay View Beach, Delaware, while the eastern shore has several shorter stretches of islands interrupted by muddy marsh shoreline.

Nearly all of the lower bay shoreline, extending north to the bay narrowing at Salem, NJ, is protected by a barrier island shoreline. Notably, the southernmost 10km of both the Delaware and New Jersey shorelines are mainland-attached barrier beaches, topped on the New Jersey side by large (10-15m) dunes. These dunes are likely relicts of previous sea level high stands (Nordstrom and Jackson, 1994). Along these southernmost reaches, salt marsh vegetation is noticeably absent and development of houses, small harbors, and other structures is quite dense. It is possible marsh fill to accommodate towns such as Lewes, Delaware and Cape May, NJ has resulted in barrier island chains merging with the mainland shore. That a similar distribution is observed in the Chesapeake Bay is not a coincidence. The shorelines nearest the bay mouth are subject to heavy development pressures for sites of urban build-up, defense, transport, farmland accessible by boat, and recreation.

The barrier islands in the lowermost parts of both the Delaware and New Jersey shorelines are consistently classic type islands, the largest, straightest, widest, and best developed of any throughout the bay (Figure 20). Not coincidentally, these islands are subject to the most intense wave climates, occasionally feeling ocean swells on the Delaware shore and receiving marine contributions to the sediment supply. Moving northward on both shorelines, the islands decrease in length, width, elevation, and sediment supply along a gradient in rough proportion to wave energy climate and normal fetch – a pattern much more evident here as compared to the Chesapeake Bay. An exception to this trend is a series of east-west trending islands, comprising Thompson's Beach and Moore's Beach on the New Jersey shoreline, that face south towards the bay entrance. These islands are the longest of any on the New Jersey (eastern) shore, and are subject to wave conditions much more energetic than west-facing neighboring islands to the southeast. The northern islands are almost entirely marsh fringe barrier islands. Two-sided islands do not exist in the Delaware Bay. As with the islands in the Chesapeake Bay, shore normal fetch is not a good predictor of island length or width. In general, though, islands with fetches exceeding 20km in the shore normal direction are classic islands; those with less than 20km fetch are marsh fringe islands.

Figure 21 & 22: A barrier island in Tangier Sound, Chesapeake Bay showing numerous overwash fans. A closeup of overwash aprons on a barrier island on the eastern shore of Chesapeake Bay.

CONTROLS ON FETCH LIMITED BARRIER ISLAND EVOLUTION

The results of this survey raise two related questions: (1) why do barrier islands exist along some bay shoreline segments and not others? (2) What will become of these islands in the future? While no simple answer exists to either question, analysis of ongoing island processes and existing knowledge of barrier island characteristics offer a perspective into island genesis and evolution.

Classic, marsh fringe, and two-sided barrier islands, like open ocean coastal plain barriers, form because they represent a stable shoreline configuration on low-slope coastal plain shorelines. These islands develop in the Chesapeake and Delaware Bays where (1) the land surface slope is low enough (2) the sediment supply great enough and (3) a topographic or vegetative nucleus exists to provide the impetus for island growth and development.

Thus islands are very numerous in the extremely low-gradient southern reaches of both bays, but do not exist along the central-western shore of the Chesapeake Bay in the vicinity of the 10m high Calvert Cliffs. In areas where barrier islands are abundant, tidal and mud flats are universally present, extending a kilometer or more offshore to the 3m contour depth. In the region of the Calvert Cliffs, the 3m contour is just 200m from shore. Likewise, much of the marsh shoreline of Tangier Sound lacks barrier islands because the sediment supply is too low or there is not adequate wave energy to push the sand onshore.

A wave-energy gradient is also responsible for the division between classic and marsh fringe islands. Greater wave energy, in part related to greater fetch, is responsible for creating longer, wider islands, and for smoothing islands into elongated sand bodies. Higher wave energy prevents vegetation from growing on the shoreface and in the inter-tidal zone. The growth of vegetation on and behind marsh fringe barrier beaches, a direct result of lower wave energy, exerts strong controls on the plan form of those islands. Proximity to the bay opening is another distinguishing characteristic between classic and marsh fringe islands, particularly in the Delaware Bay where the division is highly pronounced. Classic islands develop nearest the bay openings; marsh fringe islands develop in the lower wave energy, northern estuarine waters. Both the marine contribution to the sediment supply and wave energy are major reasons for such a division.

Sediment in the intertidal zone, nearshore system and bay bottom is rarely impacted during fair weather conditions. However, heavy seas and high winds will mobilize the sediment. As waves shoal on shore, the existing marsh grass stabilized in a peat or mud substrate reduces wave energy and induces sediment settling. Storm deposits of sediment on the salt marsh fringes of the bays and the consequential

Figure 23: A groinfield on the western shore of Chesapeake Bay near Hampton Roads. The direction of sediment transport is clearly from right to left (North to South) in the photograph.

Figure 24: A jetty at Reeds Beach, NJ in Delaware Bay shown here has trapped a significant amount of sand by the standards of fetch limited barrier islands.

overwash and future storm breaching are the primary mechanisms for island development.

These barrier islands are thus subjected to breaching and overwash with each passing storm event (Figures 21 and 22). Because subsequent fair weather conditions are inadequate to return shoreface profiles to equilibrium, sediment likely moves dominantly in the onshore direction. The Bruun Rule of shoreline response to rising sea level is thus particularly inapplicable along these low energy shorelines (Pizzuto 1985).

Erosion – better termed barrier island migration in the landward direction – is the dominant long term trend for these islands. Rosen (1980) determines that classic type islands are eroding at 0.85m/year, though with a high degree of variability (1.85 m/yr standard deviation), while marsh fringe islands are eroding at just 0.66m/yr. The lower erosion rate may be related to reduced fetch as well as to the complex interactions between fetch limited waves, the marsh platform and the presence of marsh grass on the shoreface. Pizzuto (1986) gives an erosion rate of 3m/yr for a classic transgressive barrier island along the western shore of the Delaware Bay, though this figure cannot be taken as representative for all of the barrier islands of the bay (Phillips 1986).

Stevenson *et al* (1996) describe the processes impacting island erosion and development throughout the Chesapeake Bay and conclude that antecedent topography plays an important role. They also note that shoreline evolution differs dramatically between the east and west shores of the bay. They observe an evolutionary process by which topography is drowned, becomes detached, and begins to behave as a barrier island system.

A slow but constant sea level rise is a collaborating factor, serving to augment storm surges and expedite erosion. Sea level rise alone, though responsible for loss of marsh wetlands, is unable to "drown" the barrier islands because the islands are so easily activated and are highly mobile during large storms.

Tides and aeolian processes appear to be of little importance in the long term evolution of fetch limited barrier islands within these two bays. The narrow tidal range in this region may be important in maintaining inlets and ensuring the health of backbarrier marsh communities, but likely has little impact on the overall morphology of barrier island shorelines. As dunes are rare, except for artificial ones, wind-blown sediment processes do not appear to contribute significantly to island genesis or evolution.

Given the extent of development in zones within ten kilometers of both bays' shorelines, human impact on the fetch limited barrier islands is very significant. Artificial islands are common, usually as piles of dredged sand along small channels, and were ignored in our survey. More localized influences were impossible to

Table 4: Comparison of Open Ocean and Fetch Limited Barrier Islands

	Open Ocean (Virginia & New Jersey)	Fetch Limited (Chesapeake & Delaware Bays)
Number	20+	300+
Avg. Length	>10km	1km
Avg. Width	>400m	50m
Avg. Lagoon Width	>5km	1km
Dunes	3-5m	Negligible
Maritime Forests	Dense	Negligible
Delta size (approx)	>300m^2	<100m^2
Marsh grass on beach	Rare	Common
Overwash	Important response	Dominant response
Storm waves	Significant impacts	Dominant process
Fair weather waves	Significant for alongshore transport and cross-shore stability	Negligible
Aeolian processes	Important	Negligible
Tidal dynamics	Important (many tidally-dominated)	Negligible
Response to SLR	Landward-migration or 'backstepping'	Landward-migration or 'back-stepping'
Vegetative Control	Negligible	Dominant control
Geologic Control	Primary control	Important
Human development	Dense (highrise structures)	Light (fishing shacks)

exclude. Foremost among these is the existence of extensively sea-walled shorelines throughout the bay. Many of the largest classic islands are heavily sea-walled, which has in effect "frozen" the islands in position. Jetties, groins, breakwaters, and nourishment each have associated effects on barrier island processes (Figure 23) – the cumulative impact of which may be quite significant. There is no doubt that the construction of a large jetty has adversely impacted the downdrift shorelines of Reeds Beach, NJ (Figure 24). Nourishment, an ongoing process on the western shore of Delaware Bay, has stabilized the barrier beaches, but has likely resulted in narrower than normal beaches because the islands are not permitted to overwash naturally. Indeed any human activity or development that mandates a stable shoreline imperils the barrier islands that are so heavily dependent upon being fully responsive to storms.

Because these barrier islands and their marsh lagoons are much more interdependent than open ocean barrier islands, ecological damage to the wetlands has profound implications for barrier island evolution. Marsh grass die-offs, wetland loss, ecosystem disturbance, and marsh dredging bode ill for the sustained existence of fetch limited barrier islands.

CONCLUSIONS

The important features and controls on the fetch limited barrier islands of Chesapeake and Delaware Bays can be concisely expressed as a comparison to the oceanic barrier islands of New Jersey and Virginia (Table 4).

A nearly continuous chain of oceanic barrier islands runs from Raritan Bay at the New York-New Jersey border south to Fisherman's Island at the mouth of the Chesapeake Bay. Only a 60km stretch of the Northern New Jersey and a similarly-long stretch of the Delaware and Maryland shorelines are not fronted by barrier islands (Figure 25). The twenty-two open ocean

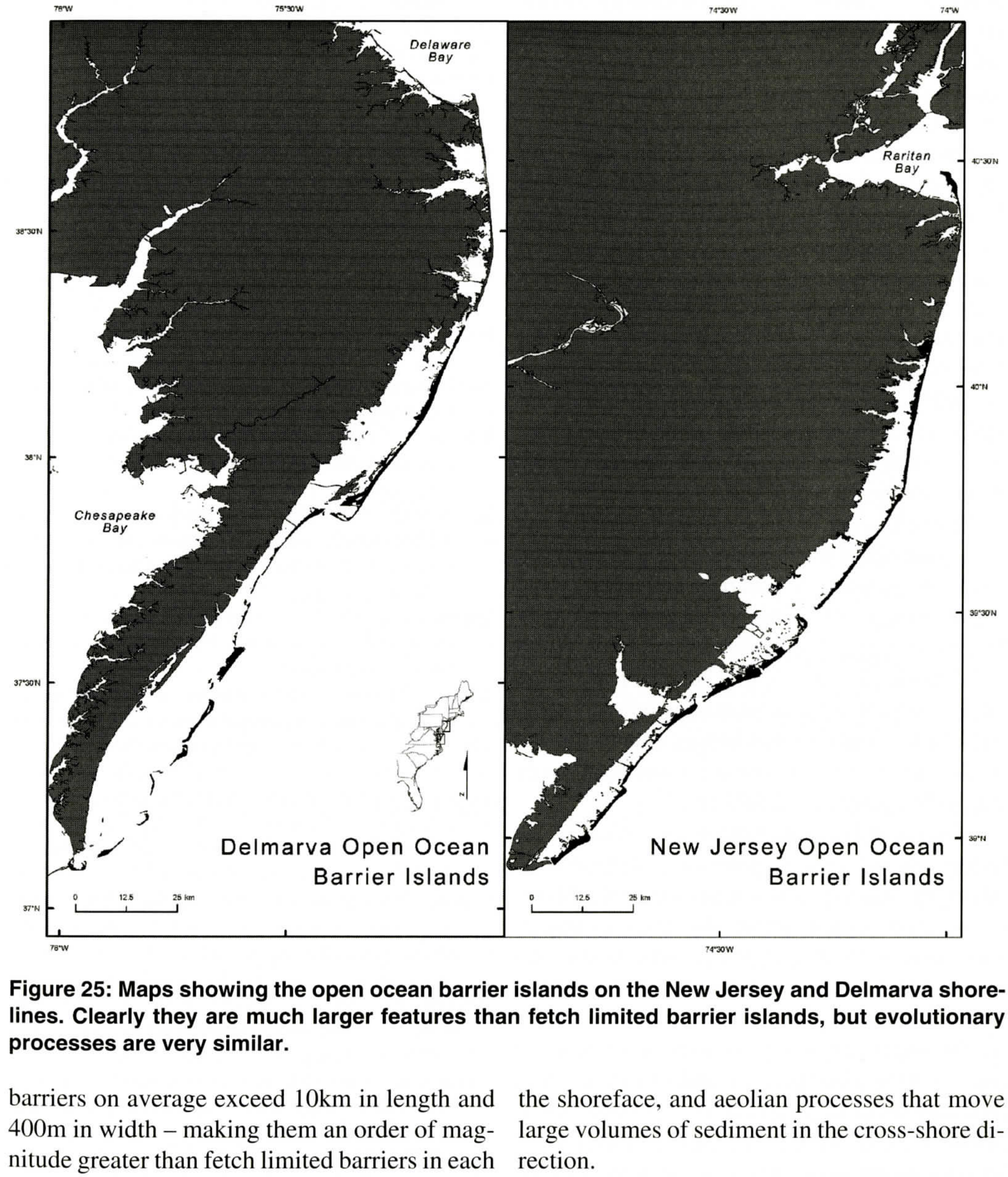

Figure 25: Maps showing the open ocean barrier islands on the New Jersey and Delmarva shorelines. Clearly they are much larger features than fetch limited barrier islands, but evolutionary processes are very similar.

barriers on average exceed 10km in length and 400m in width – making them an order of magnitude greater than fetch limited barriers in each dimension. The open ocean islands also consistently have well-developed dunes, dense maritime forests, large inlet-delta complexes, and extensive open water backbarrier lagoons, features that exist on scales far greater than those found on fetch limited barriers. Unlike fetch limited barrier islands, the open ocean islands are subject to daily, fair-weather wave processes that contribute to the alongshore flux of sediment, tidal processes that significantly impact the shoreface, and aeolian processes that move large volumes of sediment in the cross-shore direction.

Both open ocean and fetch limited barrier islands in the Mid-Atlantic are migrating landward in response to storm surges and sea level rise. The overwash and island rollover model of response to sea-level rise is attributable to islands along both ocean and estuarine shorelines. Fair weather waves operating on Atlantic coastlines after storms have passed, however, are responsible for restoring the nearshore systems to pre-storm conditions, slowing the landward movement of the island systems. However, along low energy shorelines, the absence of appreciable fair weather waves means that profiles of these islands are basically storm profiles.

Open ocean barrier islands never exhibit living marsh grass colonies on the beach and similarly are only incidentally controlled by vegetative influences such as stumps and outcropping compacted marsh mud. Geologic controls are far more important for development of barrier islands in open ocean conditions than for barrier islands in fetch limited waters (Riggs *et al* 1995). However, both types of islands require a low-sloping surface gradient, sufficient wave energy to drive sediment onshore, and a stabilizing point to serve as a nucleus.

The difference in scale between fetch limited and open ocean barrier islands is a function of differences in sediment supply and mobility and wave energy, all of which are greater in open ocean settings. That most of the component geographical features and many of the large scale controls and processes are similar, however, implies fetch limited barrier islands are but scaled down versions of the more commonly studied oceanic barrier islands.

Human-induced pressures that beset the intensely developed New Jersey coastline exist along the embayed shorelines as well. Moreover, fetch limited barrier islands are an important component in preventing wetland loss and storm damage to wetland ecosystems and human communities.

An important task for coastal scientists will be devotion of more time and efforts towards tracking the changes and behaviors of barrier islands within the Chesapeake and Delaware Bays with emphasis on the interaction of the islands and the marshes.

REFERENCES

Colman, S. M., and Mixon, R. B., 1988, The record of major quaternary sea-level changes in a large coastal plain estuary, Chesapeake Bay, Eastern United States, Palaeogeography, Palaeoclimatology, Palaeoecology, v. 68, p. 99-116.

Cooper, J.A.G. and Navas, F., 2004, Natural bathymetric change as a control on century-scale shoreline behavior, Geology, v. 32, p. 513-516.

Davis, R.A., 1994, Geology of Holocene Barrier Island Systems, 464 p.

Downs, L.L., Nicholls, R.J., Leatherman, S.P., and Hautzenroder, J., 1996, Historic Evolution of a Marsh Island: Bloodsworth Island, Maryland, Journal of Coastal Research, v. 10, p. 1031-1044.

French, J.C., 1995, Geomorphic response to sea level rise – existing evidence and future impacts, Earth Surface Processes and Landforms, v. 20, p.1-6.

Glaeser, J.D., 1978, Global distribution of barrier islands in terms of tectonic setting, Journal of Geology, v. 86, p. 283-297.

Goldsmith, V., Rosen, P., Richardson, W.S., and Sutton., C.H., 1976, Wave modeling in limited fetch basins: Making waves in Chesapeake Bay, GSA Abstracts with Programs, v. 8, p. 183.

Hardaway, C.S., Varnell, L.M., Milligan, D.A., *et al.*, 2001, Chesapeake Bay dune systems: Evolution and status, Final Report, 67 p.

Hayes, M.O., 1979, Barrier island morphology as a function of tidal and wave regime, in Leatherman, S.P (ed.) Barrier Islands: From the Gulf of St. Lawrence to the Gulf of Mexico, 325 p.

Hayes, M.O., 1994, The Georgia Bight Barrier System, in Davis, R.A. (ed.) Geology of Holocene Barrier Island Systems, p. 233-304.

Hobbs, C.H., 2004, Geological history of Chesapeake Bay, USA, Quaternary Science Reviews, v. 23, p. 641-661.

Hoyt, J.H., 1967, Barrier island formation, Geologic Society of America Bulletin, v. 78, p. 1125-1135.

Jackson, N.L., 1995, Wind and waves: influence of local and non-local ocean waves on meso-scale beach behavior in estuarine environments, Annals of the Association of American Geographers, v. 85, p. 21-37.

Jackson, N.L., Horn, D.P, Spalding, V., and Nordstrom, K.F., 1999a, Changes in beach water table elevation during neap and spring tides on a sandy estuarine beach, Delaware Bay, New jersey, Estuaries, v. 22, p. 753-762.

Jackson, N.L., 1999b, Evaluation of criteria for predicting erosion and accretion on an estuarine sand beach, Delaware Bay, New jersey, Estuaries, v. 99, p. 215-223.

Jackson, N.L., Nordstrom, K.F., Eliot, I., and Messalink, G., 2002, 'Low energy' sandy beaches in marine and estuarine environments: a review, Geomorphology, v. 48, p.147-162.

Kayan, I., and Kraft., J.C., 1971, Holocene geomorphic evolution of a barrier salt marsh system, SW Delaware Bay, Geological Society America Bulletin, v. 82, p. 2131-2158.

Knebel, H.J., 1989, Modern sedimentary environments in a large tidal estuary, Delaware Bay, Marine Geology, v. 86, p. 119-136

Kraft, J.C., Allen, E.A., Belknap, D.F., John, C.J., and Maurmeyer, E.M., 1979, Processes and morphologic evolution of an estuarine and coastal barrier system, in Leatherman, S.P (ed.) Barrier Islands: From the Gulf of St. Lawrence to the Gulf of Mexico, 325 p.

Langland, M., and Cronin, T, 2003, A summary report of sediment processes in Chesapeake Bay and Watershed USGS Water Resources Investigations Report 03-4123, 41 p.

Martinez, J.O., Gonzalez, J.L., Pilkey, O.H., and Neal, W. J., 2000, Barrier island evolution on the subsiding central Pacific Coast, Colombia, S.A, Journal of Coastal Research, v. 16, p. 663-674.

McBride, R.A., Byrnes, M.R., and Hiland, M.W., 1995, Geomorphic response type model for barrier coastlines: A regional perspective, Marine Geology v. 126, p. 143-159.

Moslow, T.F., and Heron, S.D., 1994, The Outer Banks of North Carolina, in Davis, R.A. (ed.) Geology of Holocene Barrier Island Systems, p. 47-74.

Nikitina, D.L., Pizzuto, J.E., Schwimmer, R.A., and Ramsey, K.W., 2000, An updated Holocene sea-level curve for the Delaware coast, Marine Geology, v. 171, p.7-20.

Nordstrom, K.F., 1980, Cyclic and seasonal beach response: A comparison of oceanside and bayside beaches, Physical Geography, v. 1, p. 177-196.

Nordstrom, K. F., and Sherman, D. J., 1982, Ice effects on mid-latitude marine and estuarine beaches, Northeastern Geology, v. 4, p. 134-138.

Nordstrom, K.F., and Jackson, N. L., 1990, Migration of swash zone, step and microtopographic features during tidal cycles on an estuarine beach, Delaware Bay, New Jersey, U.S.A, Marine Geology, v. 92, p. 147-154.

Nordstrom, K. F., 1992, Estuarine Beaches, New York, NY, Elsevier Science Publishing Co., 225 p.

Nordstrom, K.F., 1994a, Aeolian processes and dune fields in estuaries, Physical Geography, v.15, p. 358-371.

Nordstrom, K.F., 1994b, Developed coasts, in Carter, R.W. and C.D. Woodroffe (eds.) Coastal Evolution, 517 p.

Nordstrom, K.F., and Roman, C.T., 1996, Estuarine Shores: Evolution, Environments and Human Alterations, 486 p.

Oertel, G. F., 1985, The Barrier Island System, Marine Geology, v. 61, p. 1-18.

Oertel, G.F., and Overman, K., 2003, Sequence morphodynamics at an emergent barrier island, middle Atlantic coast of North America, Geomorphology, v. 58, p. 67-83.

Otvos, E. G., 1985, Barrier platforms: Northern Gulf of Mexico, Marine Geology, v. 63, p. 285-305

Phillips, J.D., 1986, Spatial analysis of shoreline erosion, Delaware Bay, New Jersey, Annals of the Association of American Geographers, v. 76, p. 50-62.

Pilkey, O.H., 2003, Celebration of the World's Barrier Islands, New York, NY: Columbia University Press, 309 p.

Pizzuto, J.E., 1986, Barrier island migration and onshore sediment transport, southwestern Delaware Bay, Delaware, U.S.A., Marine Geology, v. 71, p. 299-325.

Pizzuto, J.E., and Rogers, E.W., 1992, The Holocene history and stratigraphy of palustrine and estuarine wetland deposits of central Delaware, Journal of Coastal Research, v. 8, p. 854-867.

Riggs, S.R., Cleary, W. J., and Snyder, S. W., 1995, Influence of inherited geologic framework on barrier shoreface morphology and dynamics, Marine Geology, v. 126, p. 213-234.

Rosen, P.S., 1980, Erosion susceptibility of the Virginia Chesapeake Bay shoreline, Marine Geology, v. 34, p. 45-59.

Schwartz, M.L., 1973, Barrier Islands, Stroudsburg, PA, Dowen, Huchinson, and Ross, 451 p.

Smith, D., Jackson, N.L., Love, S., Nordstrom, K., *et al*, 2002, Beach Nourishment on Delaware Bay beaches to restore habitat for horseshoe crab spawning and shorebird foraging, USGS, Special Report, 51 p.

Stevenson, J.C., and Kearney, M.S., 1996, Shoreline dynamics on the windward and leeward shores of a large temperate estuary, in Nordstrom, K.F. and C.T. Roman (eds.) Estuarine Shores: Evolution, Environments and Human Alterations, 486 p.

Stutz, M.L., and Pilkey, O.H., 2002, Global Distribution and Morphology of Deltaic Barrier Island Systems, Journal of Coastal Research, Special Issue 36, p. 694-707.

Stutz, M.L., 2004, Global Distribution and Morphologic Variability of Barrier Islands, PhD Dissertation, Duke University, 304 p.

Ward, L.G., Kemp, W. M., and Boynton, W. R., 1984, The influence of waves and seagrass communities on suspended particulates in an estuarine embayment, Marine Geology, v. 59, p. 85-103.

Ward, L.G., Kearney, M.S., and Stevenson, J.C., 1998, Variations in sedimentary environments and accretionary patterns in estuarine marshes undergoing rapid submergence, Chesapeake Bay, Marine Geology, v. 151, p.111-134.

SOUTHEASTERN GEOLOGY
V. 44, No. 1, October 2005, p. 19-26

BRITTLE DEFORMATION AND FOLDING OF THE TUSCARORA SANDSTONE, WILLS MOUNTAIN ANTICLINE, WV

MICHAEL J. HARRISON[1] AND MATTHEW R. OSBORNE

Department of Earth Sciences
Tennessee Tech University
Cookeville, TN 38505

1. mharrison@tntech.edu

ABSTRACT

The Tuscarora Sandstone exposed in the core of the regional Wills Mountain anticline displays multiple smaller-scale parasitic folds. Field and thin-section observations indicate that fold-accommodation faults with small displacements (<1 m), mesoscopic deformation bands, and microfractures are more prevalent in the hinge zones of these parasitic folds when compared with the adjacent fold limbs. Detailed investigation of grain-scale brittle deformation structures across a parasitic fold indicates that deformation bands, microveins, and microcracks increase in abundance from the fold limb to the hinge zone. Microstylolites, the result of pressure solution, show no increase in abundance from the limb to hinge zone. Although both brittle and pressure-solution mechanisms were active during deformation, folding of the Tuscarora Sandstone into the Wills Mountain anticline was accomplished principally by wedge faults and microfractures operating within the hinge zones of the smaller-scale parasitic folds. The location of these parasitic folds influenced significantly the overall fold geometry of the Wills Mountain anticline.

INTRODUCTION

At Cosner Gap near Maysville, WV (Fig. 1), the Lower Silurian Tuscarora Sandstone crops out in the core of the Wills Mountain anticline, a 300+ km long, northeast-trending regional fold in the central Appalachian Valley and Ridge Province that formed over a Cambrian-Ordovician duplex during the Alleghanian orogeny (Perry, 1978; Kulander and Dean, 1986; Mitra, 1986; Wilson and Shumaker, 1988; Ferrill and Dunne, 1989; Smart *et al.*, 1997). The Tuscarora Sandstone is a medium- to coarse-grained, well-sorted quartz arenite 25-60 meters thick that, because of its mechanical competency, acts as a primary lithotectonic unit in the roof sequence of Ordovician to Pennsylvanian strata in the Valley and Ridge Province (Jacobeen and Kanes, 1975; Wiltschko and Chapple, 1977; Evans, 1989).

On the north side of Cosner gap, the Tuscarora Sandstone contains four discrete parasitic folds with chevron-like hinge zones separated by relatively planar fold limbs (Fig. 2). Field observations indicate that these hinge zones are not located near fold-related faults in the underlying Juniata Formation or the overlying Clinton Group. Previous research has shown that outcrop-scale folds in the central Appalachians commonly display angular fold hinges (e.g., Faill, 1973; Narahara and Wiltschko, 1986; Dunne, 1996). However, it remains unclear how regional folds (like the Wills Mountain anticline) that contain multiple small-scale fold hinges achieve their fold geometry. This study aims to understand the deformation mechanisms that localized the parasitic folds across the Wills Mountain anticline.

METHODS

Nine oriented samples of Tuscarora Sandstone were collected from the same stratigraphic horizon across a parasitic fold on the northwest-dipping limb of the anticline (Fig. 2). This fold was selected because it displays a

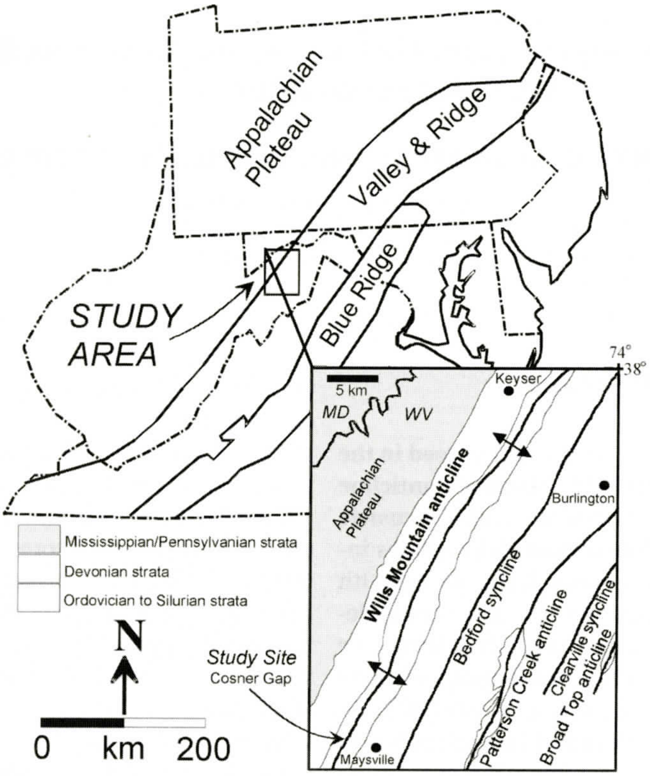

Figure 1. Regional map showing the geology and physiographic provinces. The study site is located in the core of the Wills Mountain anticline, WV.

~25° dip change in bedding over a short arc length of the anticline (Table 1). Although only the parasitic fold on the northwest-dipping limb was sampled, station mapping was performed over the entire anticline to document outcrop-scale deformation bands and wedge faults, especially in the hinge zones of the other parasitic folds. Collected samples were cut into three mutually perpendicular thin sections (parallel to bedding, normal to bedding/normal to bedding strike, normal to bedding/parallel to bedding strike) to assess the abundance of microstructures. Sample 12 was collected as an unoriented sample and, thus, only its bulk microstructure density was reported. Because microstructures often indicate which deformation mechanisms were operative (Groshong, 1988; Knipe, 1989), their abundance and spatial variation may be used to determine the relative importance of different mechanisms within a folded layer.

Table 1. Bedding attitude across a parasitic fold on the northwest-dipping limb of the Wills Mountain anticline. See Figure 2 for station locations.

Station	Strike/Dip of Bedding
9	047/10 NW
10	042/10 NW
11	045/15 NW
12	021/34 NW
13	021/34 NW
14	044/34 NW
15	026/38 NW
16	026/38 NW
17	024/56 NW

The Tuscarora at Cosner Gap displays brittle and pressure-solution microstructures. The brittle microstructures used for this study include deformation bands (cataclastic zones ~10 μm to several mm wide), microveins (~10-200 μm wide), and microcracks (marked by fluid-inclu-

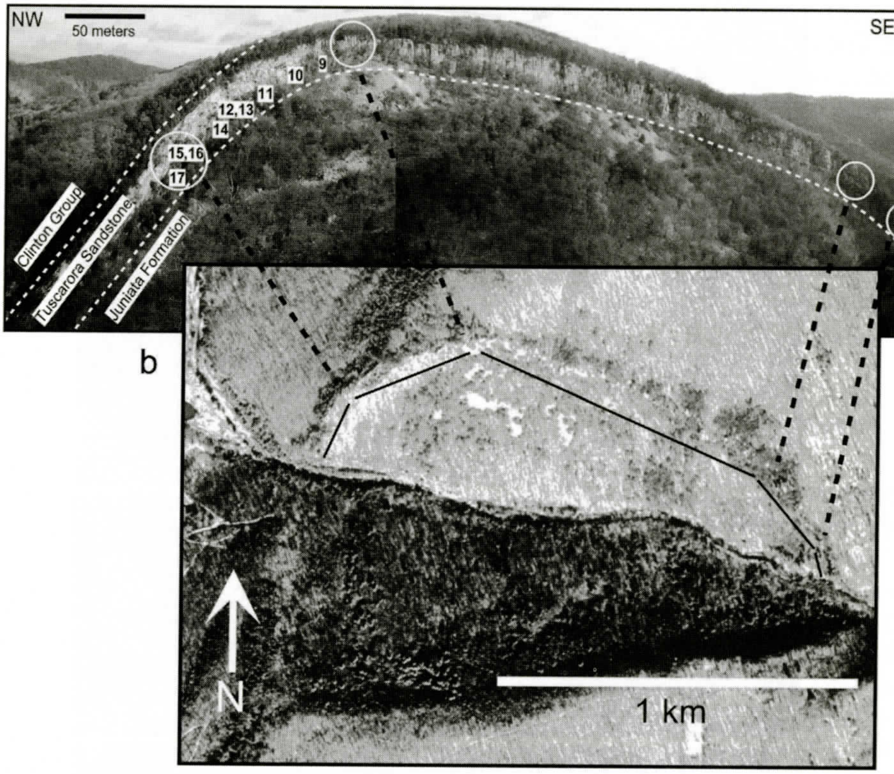

Figure 2. (a) The Wills Mountain anticline at Cosner Gap, WV (view to the northeast). On the north side of Cosner Gap, the Wills Mountain anticline displays four parasitic folds (indicated by circles). Numbers correspond to sample sites. (b) Air photo of Cosner Gap showing the parasitic folds that comprise the Wills Mountain anticline. Solid line segments in (b) parallel fold-limb zones. Dashed lines connect the parasitic folds in (a) and (b).

sion planes ~0.5-5 μm wide). Microstylolites were used to infer pressure solution (microstructure terminology after Blenkinsop, 2000). Only transgranular microstructures (crosscutting cement and framework grains) were used in this study to ensure the evaluation of *in situ* deformation microstructures and not inherited structures (see Onasch and Dunne, 1993; Onasch *et al.*, 1998). A petrographic microscope was used to identify and quantify the abundance of the microstructures; cathodoluminescence microscopy identified microveins. The microstructure density (the number of microstructures intersecting a unit line length) was used to compare samples across the fold. For each of the nine samples, a mean microstructure density was calculated from the three thin sections cut from that sample.

RESULTS

Outcrop-Scale Structures

Four parasitic folds were identified in the Tuscarora on the north side of Cosner Gap (Fig. 2). The hinges of these parasitic folds trend subparallel to the trend of the larger Wills Mountain anticline (oriented ~030°). Mapping at station locations across the anticline revealed few fracture zones or faults with large displacements (>1 m) (Fig. 3a). In fact, none of the parasitic folds is associated with large fold-related faults. Competent rock units commonly contain fold-accommodating wedge faults that form in the hinge and limbs (Cloos, 1964; Mitra, 2002). At Wills Mountain, the wedge faults near the parasitic hinges commonly display small dis-

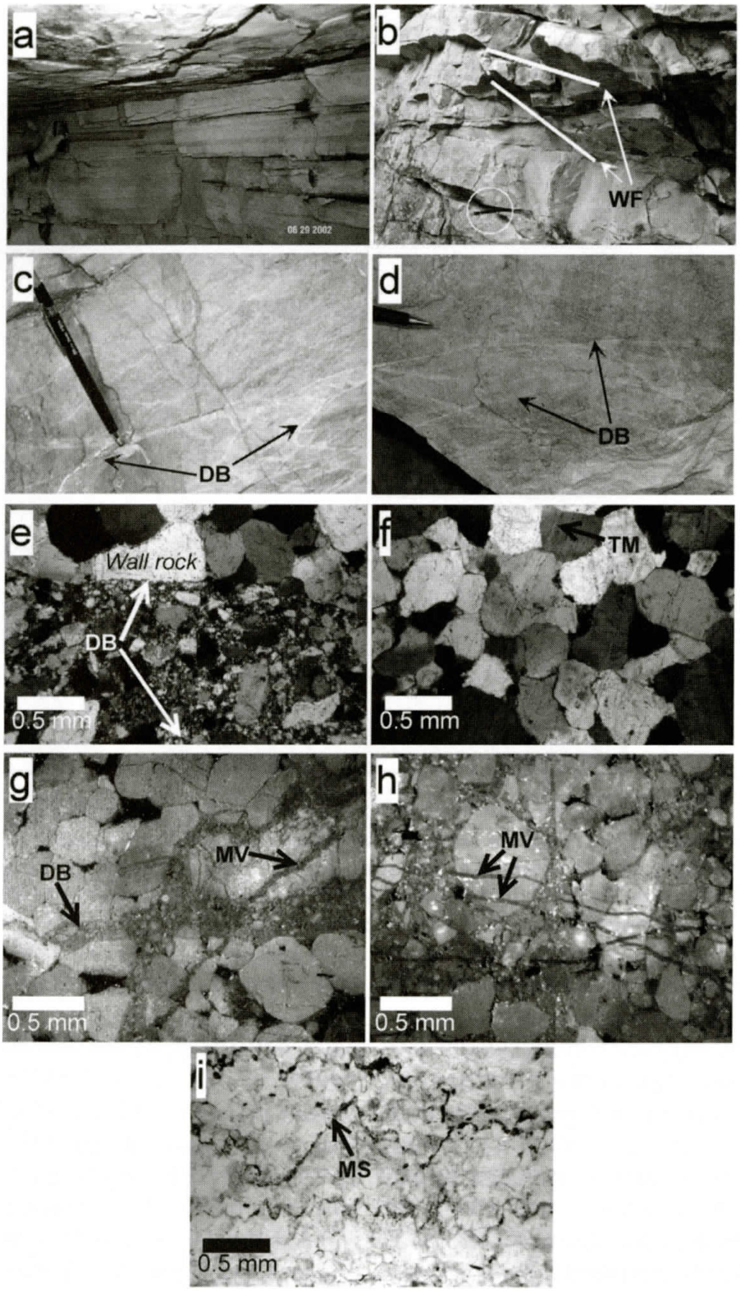

Figure 3. Outcrop photos and photomicrographs of deformation microstructures in the Tuscarora Sandstone. (a) Sample site 11 (parasitic limb-zone) showing no outcrop-scale deformation structures. Rock hammer for scale. See Figure 2 for sample locations. (b) Wedge faults (WF) at sample site 12 closer to parasitic hinge. White lines parallel fault surface. Pencil for scale (circled). (c and d) Sample sites 14 and 15 showing deformation bands (DB) that appear as thin white bands. Pencil for scale. (e) Deformation band with wall rock above. (f) Transgranular microcracks (TM). (g) Deformation band and microvein (MV). (h) Microveins. (i) Microstylolite (MS). Photomicrographs (e) and (f) taken with cross-polarized light; (i) taken with plane-polarized light. Photomicrographs (g) and (h) are cathodoluminescence images.

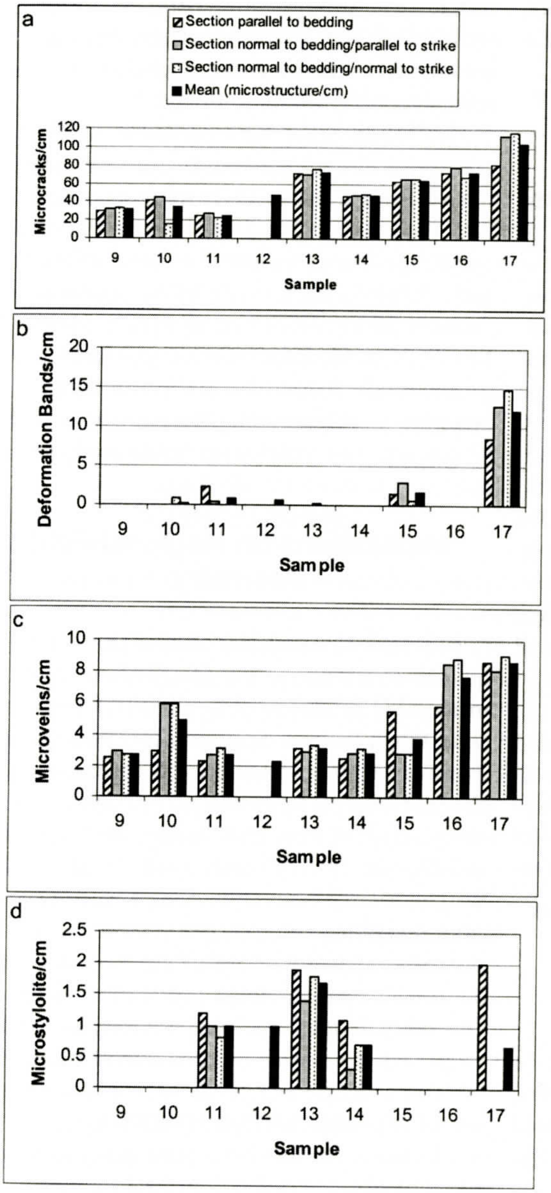

Figure 4. Microstructure density for the three thin sections prepared from each sample. Mean density shown as black bars. (a) microcracks; (b) deformation bands; (c) microveins; and (d) microstylolites. Legend in (a) applies to all figures. Samples 15-17 are located in the hinge zone of the parasitic fold (see Figure 2). Sample 12 collected as an unoriented sample.

placements (<1 m) (Fig. 3b). These faults are commonly associated with deformation bands (Fig. 3c-d). In the hinge zones, deformation bands typically form anastomosing swarms or tabular conjugate sets that dip at a low angle (<30°) to bedding. Both wedge faults and deformation bands increase in abundance from parasitic limb to hinge zones. The scarcity of slickenlines or slickenfibers on the bedding surfaces across the anticline suggests minimal flexural shear during folding.

Grain-Scale Structures

Microstructures indicate that brittle deformation (Fig. 3e-h) and pressure solution (Fig. 3i) were the dominant grain-scale mechanisms active during deformation. Crystal-plasticity microstructures (e.g., undulatory extinction, kink bands, and deformation lamellae) accommodated only a small fraction of the finite strain (~1%), thus these structures were ignored in this study (see Harrison and Onasch, 2000). Brittle-deformation microstructures including deformation bands, microveins, and microcracks increase in mean density from parasitic fold limb to hinge (Fig. 4a-c). Interestingly, sections cut normal to bedding/normal to strike generally show greater microfracture density in the hinge zone. A possible explanation for this observation is that this section shows deformation related to both deposition-related compaction and shear associated with layer-parallel shortening and folding. Other studies have also noted greater microstructure abundance in sections cut with this orientation (e.g., Onasch, 1990; Harrison and Onasch, 2000).

Microstylolites show no increase in density from fold limb to hinge zone; however, slightly greater clay content in samples 11-14 may account for their presence locally (Fig. 4d). Most microcracks, microveins, and microstylolites are oriented approximately (1) parallel to bedding, (2) normal to bedding/parallel to bedding strike, and

(3) normal to bedding/normal to bedding strike. Deformation bands generally parallel the bedding strike and dip at a low angle to bedding.

DISCUSSION

Chronology of Deformation Events

Deformation of the Tuscarora Sandstone at Wills Mountain followed a sequence of deposition and compaction, cementation, layer-parallel shortening and then folding, as determined by crosscutting relations and from previous studies in the region (e.g., Sibley and Blatt, 1976; Onasch, 1990; Onasch and Dunne, 1993; Onasch *et al.*, 1998; Harrison and Onasch, 2000). Pressure solution was the dominant mechanism during compaction, forming bed-parallel stylolites. After cementation, bed-normal stylolites, transgranular microfractures, and mesoscopic deformation bands developed mainly in the hinge zones due to layer-parallel shortening and folding (Harrison and Onasch, 2000). Strain-partitioning analysis for folded Tuscarora near Keyser, WV (see Fig. 1) indicates that pressure solution resulted in 25% layer-normal shortening and 10% layer-parallel shortening at the grain scale (Harrison and Onasch, 2000).

Spatial Variation of Brittle Structures

Stations spaced across the anticline show that wedge faults and outcrop-scale deformation bands increase in abundance from fold limbs to hinge zones of the parasitic folds; microfracture densities show a similar distribution (Fig. 4). Although the microfracture densities likely include some microfractures that formed prior to folding (e.g., during compaction, layer-parallel shortening, or even pre-Alleghanian tectonics), the increase in abundance in the parasitic hinge zone, we argue, reflects the effects of Alleghanian deformation, as suggested by the coaxial orientation of the parasitic folds with the larger Wills Mountain anticline—a known Alleghanian structure (e.g., Perry, 1978; Dunne, 1996). We assume that the pre-folding brittle structures were distributed uniformly within the Tuscarora; thus, any increase in abundance in the parasitic hinge zone is likely related to Alleghanian folding.

Our results agree with previous studies that concluded that microfracturing dominated during the folding of the Tuscarora (or its correlative, the Massanutten Sandstone) in the Valley and Ridge (Narahara and Wiltschko, 1986; Onasch, 1990; Onasch *et al.*, 1998; Harrison and Onasch, 2000). However, this study further illustrates that the formation and geometry of regional-scale folds like the Wills Mountain anticline is influenced by the collective action of outcrop- and grain-scale brittle mechanisms operating within parasitic folds.

Implications for Regional-Fold Geometry

Previous research has shown that roof-sequence strata above the Martinsburg detachment in the central Appalachians lack regional-scale thrust faults with large displacements and that most of the Alleghanian deformation was accommodated by outcrop- and grain-scale mechanisms (Evans and Dunne, 1991; Onasch and Dunne, 1993; Dunne, 1996; Markley and Wojtal, 1996). Moreover, Smart *et al.* (1997) determined that outcrop- and grain-scale mechanisms account for ~75% of the roof-sequence deformation in the vicinity of Wills Mountain. Our study demonstrates that not only does outcrop- and grain-scale deformation dominate in the Tuscarora (in fact, no large thrusts were observed anywhere across the fold), but that brittle mechanisms are localized principally in hinge zones of parasitic folds. It is the localization of these brittle-deformation mechanisms in the Tuscarora that produced the parasitic folds; consequentially, these parasitic folds accommodated much of the deformation and thus influenced the overall regional-scale geometry of the Wills Mountain anticline at Cosner Gap.

Arguably, the Tuscarora Formation is the stiff lithotectonic unit that most influences regional-scale fold geometry in roof-sequence strata. At Cosner Gap, the Tuscarora displays four discrete parasitic folds not associated with large fold-related faults in the adjacent formations. Thus, although the regional Wills Mountain anticline formed over a Cambrian-Ordovician duplex (e.g., Wilson and Shumaker, 1992) the location of the parasitic folds in the Tuscarora may be solely the result of intraformational textures and/or heterogeneities. Preliminary results by Osborne *et al.* (2003) suggest that lateral variations in cementation or porosity in the Tuscarora, perhaps associated with changes in facies, may have localized the parasitic folds at Cosner Gap. Thus, the brittle-deformation microstructures in the hinges of these parasitic fold hinges may have been preferentially located by rock texture.

CONCLUSIONS

Field and thin-section observations indicate that outcrop- and grain-scale brittle deformation within parasitic fold hinges accommodated folding of the Tuscarora Sandstone in the Wills Mountain anticline at Cosner Gap, WV. Our results agree with previous studies that indicate that mesoscopic and small-scale mechanisms dominated the deformation in roof-sequence strata of the central Appalachians (e.g., Dunne, 1996; Smart *et al.*, 1997). The absence of major fold-related faults within the Tuscarora or adjacent formations suggests that intraformational heterogeneities or rock texture may have influenced the location of the parasitic folds and, thus, the overall fold geometry of the Wills Mountain anticline.

ACKNOWLDGEMENTS

The authors thank Charlie Onasch, Bill Dunne, and Ed Simpson for their assistance in the field and for their helpful discussions. Steve Whitmeyer and an anonymous reviewer greatly improved the content of this manuscript. The research was supported by NSF grant EAR-0087607.

REFERENCES

Blenkinsop, T., 2000, Deformation microstructures and mechanisms in minerals and rocks: Dordrecht, Kluwer Academic Publishers, 150 p.

Cloos, E., 1964, Wedging, bedding plane slips, and gravity tectonics in the Appalachians, *in* Lowry, W.D., ed., Tectonics of the Southern Appalachians: Virginia Polytechnic Institute and State University Department of Geological Sciences Memoir 1, p. 63-70.

Dunne, W. M., 1996, The role of macroscale thrusts in the deformation of the Alleghanian roof sequence in the central Appalachians: A reevaluation: American Journal of Science, v. 296, p. 549-575.

Evans, M. A., 1989, The structural geometry and evolution of foreland thrust systems, northern Virginia: Geological Society of America Bulletin, v. 101, p. 339-354.

Evans, M. A. and Dunne, W. M., 1991, Strain factorization and partitioning in the North Mountain thrust sheet, central Appalachians, U.S.A.: Journal of Structural Geology, v. 13, p. 21-35.

Faill, R. T., 1973, Kink-band folding, Valley and Ridge Province, Pennsylvania: Geological Society of America Bulletin, v. 84, p. 1289-1314.

Ferrill, D. A. and Dunne, W. M., 1989, Cover deformation above a blind duplex: An example from West Virginia, U.S.A.: Journal of Structural Geology, v. 11, p. 421-431.

Groshong, R. H., 1988, Low-temperature deformation mechanisms and their interpretation: Geological Society of America Bulletin, v. 100, p. 1329-1360.

Harrison, M. J. and Onasch, C. M., 2000, Quantitative assessment of low-temperature deformation mechanisms in a folded quartz arenite, Valley and Ridge Province, West Virginia: Tectonophysics, v. 317, p. 73-91.

Jacobeen, F. and Kanes, W. H., 1975, Structure of Broadtop synclinorium, Wills Mountain anticlinorium, and Allegheny frontal zone: American Association of Petroleum Geologists Bulletin, v. 59, p. 1136-1150.

Kulander, B. R. and Dean, S. L., 1986, Structure and tectonics of central and southern Appalachian Valley and Ridge and Plateau Provinces, West Virginia and Virginia: American Association of Petroleum Geologists Bulletin, v. 70, p. 1674-1684.

Knipe, R. J., 1989, Deformation mechanisms—recognition from natural tectonites: Journal of Structural Geology, v. 1, p. 127-146.

Markley, M. and Wojtal, S., 1996, Mesoscopic structure, strain and volume loss in folded cover strata, Valley and Ridge Province, Maryland: American Journal of Science, v. 296, p. 23-57.

Mitra, S., 1986, Duplex structures and imbricate thrust systems: Geometry, structural position, and hydrocarbon potential: American Association of Petroleum Geologists Bulletin, v. 70, p. 1087-1112.

Mitra, S., 2002, Fold-accommodation faults: American Association of Petroleum Geologists Bulletin, v. 86, p. 671-693.

Narahara, D. K. and Wiltschko, D. V., 1986, Deformation in the hinge region of a chevron fold, Valley and Ridge Province, central Pennsylvania: Journal of Structural Geology, v. 8, p. 157-168.

Onasch, C. M., 1990, Microfractures and their role in deformation of a quartz arenite from the central Appalachian foreland: Journal of Structural Geology, v. 12, p. 883-894.

Onasch, C. M. and Dunne, W. M., 1993, Variation in quartz arenite deformation mechanisms between a roof sequence and duplexes: Journal of Structural Geology, v. 15, p. 465-475.

Onasch, C. M., Shen-Tu, B. and Couzens-Schultz, B. A., 1998, Strain partitioning and factorization in a quartz arenite: Journal of Structural Geology, v. 20, p. 1065-1074.

Osborne, M. R., Harrison, M. J., Onasch, C. M. and Dunne, W. M., 2003, The influence of primary sedimentary features on fold-hinge development in quartz arenite deformed at low temperature: Geological Society of America Abstracts with Programs, v. 35, no. 6, p. 178.

Perry, W. J., 1978, The Wills Mountain anticline: a study in complex folding and faulting in eastern West Virginia: WV Geologic and Economic Survey, No. RI-32.

Sibley, D. F. and Blatt, H., 1976, Intergranular pressure solution and cementation of the Tuscarora orthoquartzite: Journal of Sedimentary Petrology, v. 46, p. 881-896.

Smart, K. J., Dunne, W. M. and Krieg, R. D., 1997, Roof sequence response to emplacement of the Wills Mountain duplex: the roles of forethrusting and scales of deformation: Journal of Structural Geology, v. 19, p. 1443-1459.

Wilson, T. H. and Shumaker, R. C., 1988, Three-dimensional structural interrelationships within Cambrian-Ordovician lithotectonic unit of central Appalachians: American Association of Petroleum Geologists Bulletin, 72, 600-614.

Wilson, T. H. and Shumaker, R. C., 1992, Broad Top thrust sheet: an extensive blind thrust in the central Appalachians: American Association of Petroleum Geologists Bulletin, v. 76, p. 1310-1324.

Wiltschko, D. V. and Chapple, W. M., 1977, Flow of weak rocks in Appalachian Plateau folds: American Association of Petroleum Geologists Bulletin, 61, 180-197.

SOUTHEASTERN GEOLOGY
V. 44, No. 1, October 2005, p. 27-36

AN INVESTIGATION OF JOINT SETS AND THEIR RELATION TO OCCURRENCES OF RARE BIOTA AT THE BROXTON ROCKS PRESERVE, ALTAMAHA FORMATION (MIOCENE), COFFEE COUNTY, GEORGIA

LUKE A. DAVIS

Department of Earth Sciences
University of North Carolina Wilmington
Wilmington, NC 28403-3201
lad5290@uncw.edu

FREDRICK J. RICH

Department of Geology and Geography
Georgia Southern University
Statesboro, GA 30460-8149
frich@georgiasouthern.edu

ABSTRACT

The Broxton Rocks Preserve, located in northern Coffee County, Georgia, is owned by The Nature Conservancy (TNC). It occupies a portion of the Atlantic Coastal Plain where Miocene strata dip gently eastward. "The Rocks" are erosional remnants of the Altamaha Formation, and exhibit outcrops that are up to 6 m high that contain numerous sub-vertical and vertical joints. Erosion has widened a few of the joints in excess of a meter. Four joint orientations are dominant: two major sets, 1) 015°-195° +/- 15° (NE-SW set) and 2) 095°-275° +/- 15° (E-W set), and two minor sets 3) 130°-310° +/- 10° and 4) 155°-335° +/- 10° (NW-SE set). The large joints on the topographic surface show that the E-W joints (095°-275°) are older than a weak N-S set (355°-175°), while the NW set (155°-335°) appears to be the oldest set. Rocky Creek, a first-order ephemeral stream, dissects part of the outcrops and flows in a rectilinear pattern from its knick point at Rock Falls. Orientations of the stream channel segments mimic those of the joints, but with a more dominant NW-SE trend (155°-335°).

Broxton Rocks contains over 500 species of plants; some are very rare. Though the outcrops are dominated by longleaf pine and numerous xeric species, the range of microclimates provided by the different joint sets is conducive to the growth of such unusual plants as filmy ferns, shoestring ferns, and green-fly orchids. Diverse animal species inhabit the varied landscape as well, including gopher tortoises, indigo snakes, eastern woodrats, flying squirrels, and a variety of birds. Both the geology and natural communities of Broxton Rocks are unusual in southern Georgia.

INTRODUCTION

Broxton Rocks is a unique natural landscape integrated with diverse plant and animal communities where geologic factors appear to have promoted the development of habitable niches for a wide variety of organisms. This study presents the results of physical examination of joints that typify Broxton Rocks. We discuss how the joints have shaped the course Rocky Creek and how they have influenced the ecology of Broxton Rocks.

GEOLOGIC SETTING

The Broxton Rocks Preserve is approximately 15 highway kilometers (9.3 mi) north of Broxton (pop.1460) in northeastern Coffee County, Georgia. Coffee County is located in

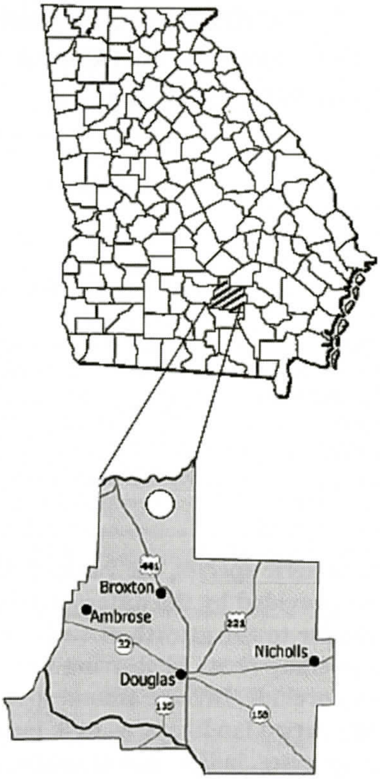

Figure 1. Location of the study area. White circle on lower image indicates the location of Broxton Rocks Preserve.

the southern part of the state in the Coastal Plain, approximately 110 km (70 mi) north of the Georgia-Florida border (Figure 1). Rocky Creek flows through the property and is closely associated with the development of the "Rocks." Where the stream cascades over the exposure of the Altamaha Formation (Miocene), it forms Rock Falls, located on the Broxton NE 7.5-minute quadrangle, and lying in the core of the 2000-acre property owned by TNC (Figure 2).

Broxton Rocks is composed mostly of quartzose sandstone, a part of the Altamaha Formation previously named the "Altamaha Grit" by Dall and Harris (1892) (Figure 3). According to Huddlestun (1988), the Altamaha Formation is a laterally extensive Miocene formation composed primarily of a pebbly, clayey sand. Quartz and kaolinite are the two most common mineral constituents, but illite, smectite, and

Figure 2. Rock Falls, a 2-meter waterfall, located in the Broxton Rocks Preserve. The falls serves as a geomorphic knick point for Rocky Creek.

iron oxide nodules occur as minor components. Many of these minerals are found on the numerous joint faces in the formation, and iron oxides commonly stain rock faces.

Figure 3. A typical outcrop of the Altamaha Formation at Broxton Rocks in March, 2003. Person is 1.8m in height.

The absence of fossils, the thick beds with occasional cross-bedding, and abundant rounded quartz pebbles suggest a high-energy fluvial or estuarine environment of deposition. An extensive part of the Altamaha Formation occurs in the NE-trending Gulf Trough, which is generally interpreted as a scour feature caused by a paleoocean current similar to the Gulf Stream; the trough served as a site of deposition for the Altamaha Formation in the Oligocene and Miocene (Huddlestun, 1988). The Altamaha Formation disconformably overlies numerous formations in Georgia, including the Tobacco Road, Ocmulgee, Parachula, and Coosawhatchie Formations (Huddlestun, 1988) and its resistant sandstone units cap topographically high areas in the region.

ECOLOGY

Biological and ecological surveys of Broxton Rocks show that the associated flora and fauna are quite unusual and include species that are rare, not only in Georgia, but in the world (Snow, 1994). Mr. Frankie Snow of South Georgia College in Douglas, Georgia, has maintained a diversity inventory of the Broxton Rocks Preserve for many years. As of June 2002, over 530 species of vascular plants, 150 species of bryophytes (including mosses, liverworts, and hornworts), and 150 lichen species were identified in this small watershed (45 km^2 or 17mi^2) (F. Snow, personal communication 2003). A number of the more unusual plants, including the green-fly orchid (*Epidendrum conopseum*), dwarf filmy fern (*Trichomanes petersii*), and shoestring fern (*Vittaria lineata*) occupy the narrow, moist defiles provided by joint sets. Other rare plant species such as grit portulaca (*Portulaca biloba*), cutleaf beardtongue (*Penstemon dissectus*), and pineland barbara buttons (*Marshallia ramosa*) populate only the sunny regions on the horizontal surfaces of the outcrops at Broxton Rocks (Snow, 1994). The fauna at Broxton Rocks includes 100 species of birds, 30 reptile and amphibian species, and 20 species of mammals. According to Snow (1994), the more distinctive faunal species include gopher tortoises (*Gopherus polyphemus*), indigo snakes (*Drymarchon corais couperi*), eastern woodrats (*Neotoma floridana*), and flying squirrels (*Glaucomys volans*). Since many of these species occupy specific niches encroached upon by anthropogenic influences, over 30 plant and animal species are globally ranked as rare (Snow, 1994). The high level of biodiversity and the rarity of certain species at Broxton Rocks are the primary reasons that the property was purchased by TNC in 1992. Incorporating the property into a 2000-acre tract was intended to secure a safe future for the land and its unique biological communities.

Figure 4. A map view of two large outcrop-dissecting joints with north at the top edge of the figure. The E-W joint (098°-278°) extends left to right across the figure is older than the N-S joint (005°-185°) because the N-S joint truncates into the E-W joint. Note photo scale.

JOINTS

Sedimentary rocks of the Coastal Plain in Georgia were deposited on a passive margin, an area not associated with a major plate boundary (Huddlestun, 1988). Although these Mesozoic and younger strata never have been deeply buried, tectonic joints have developed within the Coastal Plain of Georgia and South Carolina (Figure 4). The origin of the joints and the associated stress regimes is ambiguous and will be discussed later in the paper.

Joints are planar surfaces along which little displacement has occurred and opening of joints is usually perpendicular to the joint surface. Joints commonly occur in sets that display preferred orientations. Age relationships generally can be determined in the field by identifying the truncation of one joint set into another. However, the investigator must fully understand the stresses and sequence of deformational episodes in the region to be absolutely confident in their age relationships.

Numerous joints at a variety of scales exist in the Miocene sandstone at Broxton Rocks. Bartholomew and others (2000) collected data near the Georgia and South Carolina coast and along the Savannah River, but data from south-central Georgia were lacking. Because of the proximity of Broxton Rocks to the Savannah River, our data are compared with those of Bartholomew and others (2000).

Despite limited occurrences of suitable study areas, research has been conducted on Coastal Plain joints and includes the study of joint sets in Miocene and younger strata of the lower Coastal Plain (Bartholomew and others, 2000). Many of these joint sets exhibited a 065°-245° strike that is consistent with the inferred regional 63° strain-direction associated with earthquakes near Charleston, South Carolina (Bartholomew and others, 2000). Blanchard and others (1997) studied extensional joints in the Altamaha and Tobacco Road Formations on the Savannah River Site. Four joint sets were identified with orientations (from oldest to youngest): 1) 125°-295° +/-15°, 2) 165°-345° +/-15°, 3) 095°-275° +/-15°, and 4) 035°-225° +/-15°. Blanchard and others (1997) suggest that the second and fourth joint sets are related to Late Eocene-Miocene extensional movement of two faults near the Savannah River Site.

Joint data have also been collected in the Gulf Coastal Plain, especially in Louisiana. Washington (2003) described three pairs of joint sets in Eocene-age strata adjacent to river valleys in northern Louisiana. Two pairs of younger joint sets trend 005°-185°/085°-265° and 025°-205°/100°-280° and an older pair trends 060°-240°/145°-325° (Washington, 2003). Washington (1998) suggested that regionally consistent orientations, morphologies, and age relationships of the joint systems in northwestern Louisiana were caused by regional tectonic events. McCulloh (2003) proposed that rectilinear drainage patterns throughout Louisiana are due to fractures in the underlying lithologies. A rose diagram of 100-m stream segments (n=289,383 identified exclusively from digital data) was plotted and three dominant trends were observed: 1) 000°-180°, 2) 155°-335° +/-5°, and 3) 095°-275° +/-5° (McCulloh, 2003).

Other research has focused on the seismicity, deformation, and various lithologies of the southern Atlantic Coastal Plain. Talwani (1997) has studied neotectonic activity, both past and present, on the Ashley River Fault near Charleston, South Carolina. Seismic activity associated with this fault resulted in an earthquake in 1886 (moment magnitude 7.3) that was responsible for damage or destruction of buildings and other cultural features as well as 100 fatalities (Dutton, 1889). It also produced joints in some surficial Holocene sediments (Dutton, 1889). Based on a large database derived from structural measurements, Bartholomew and others (1997) suggested that four different stress regimes have produced the joints visible throughout the Georgia-South Carolina Coastal Plain and that alternating periods of extension and compression in preferred directions caused the formation of joint sets. Smith (1983) investigated the basement geology of the Florida panhandle and discovered two normal faults that strike 040°-220° and 130°-310°. These basement faults could have propagated stress to the overlying strata.

STUDY SITE

The study area contains many joints, which vary greatly in scale from millimeters to tens of meters in length. Rocky Creek flows in a rectilinear pattern between the sandstone cliffs, and most likely facilitated the erosional and weathering processes that created the outcrops (Figure 5). Rock Falls is located at 31.732° N and 82.853° W, and is a geomorphic knick point in the Rocky Creek watershed (Figure 2). As time has progressed, the creek has eroded headward into the sandstone, thus Rock Falls has migrated to the south. The valley between the sandstone cliffs on either side of Rocky Creek increases from 30 m (164 ft) at the falls to over 140 m (460 ft) 600m (1,969 ft) downstream of the falls. Figure 6 illustrates this point. The valley continues to widen as you progress downstream to almost 400 m (1,312 ft) one mile downstream of the falls.

Figure 5. This image of Rocky Creek was taken from the top of an outcrop with north as the lower right corner of the figure. Rocky Creek is a northward-flowing, ephemeral first-order stream that exhibits a rectilinear pattern through Broxton Rocks.

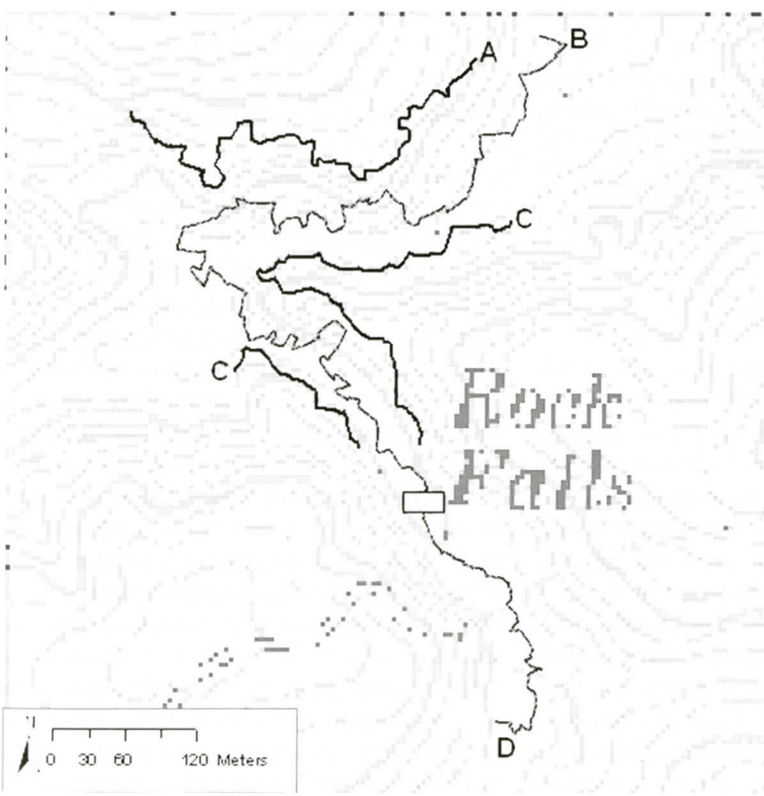

Figure 6. A map of the study area created using ArcMap GIS. The rectangle represents the location of Rock Falls. A: Small outcrop, B: Rocky Creek downstream of Rock Falls, C: Large outcrop, and D: Rocky Creek upstream of Rock Falls. Note the rectilinear drainage pattern downstream of Rock Falls (B). The fainter lines represent the original contour lines from the USGS Broxton NE 7.5-minute quadrangle.

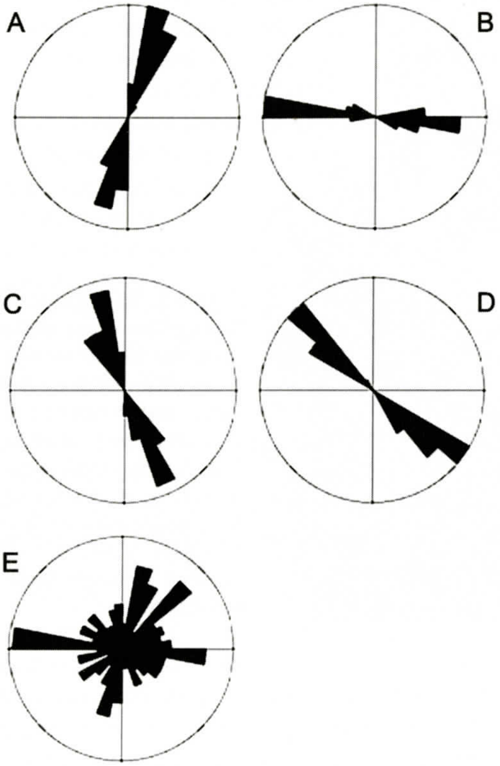

Figure 7. Equal-area rose diagrams of joints measured at Broxton Rocks. A: 015°-195° +/- 15°, 76 joints (circle- 22%); B: 095°-275° +/- 15°, 79 joints (28%); C: 155°-335° +/- 10°, 40 joints (22%); D: 130°-310° +/- 10°, 36 joints (25%); E: 321 joints (7%) in the outcrops at Broxton Rocks.

METHODS

Attitudes, lengths, widths, and heights of 321 joints were measured using Brunton and Sylva compasses implementing the right-hand rule (Freeman, 1999). The right-hand rule is a convention establishing strike and dip of geologic structures. When using the right-hand rule, the researcher must place his right hand palm up, open and extended, with the thumb pointing in the down-dip direction; the direction of the fingertips provides the strike of the structure (Freeman, 1999). Since over 90 percent of the dips exceeded 75 degrees, the joints are classified as sub-vertical. The trends of 101 channel segments of Rocky Creek were measured by sighting downstream along the channel centerline. All strikes and trends were recorded using azimuths. Age relationships were determined in the field on several joints of varying lengths. The age relationships were identified readily because younger joints terminate against older ones.

The strikes of the joints and trends of the stream channels were plotted as rose diagrams using Stereonet 6.0.2, a Macintosh-based program written by Richard Allmendinger of Cornell University (Figure 7a-d). A Trimble Geoexplorer 3 Global Positioning System (GPS) unit and a Beacon-On-a-Belt were used to map the outcrops and a substantial segment of Rocky Creek. The raw data were downloaded into Pathfinder software and corrected to improve accuracy. Data correction was preformed manually and using the program's correction command. This was necessary to eliminate outlying points caused by poor satellite geometry during data collection. Using the corrected data, Figure 6 was created using ArcMap GIS software.

RESULTS

Stream-course trends (n=101) and joint strikes (n=321) were plotted on separate rose diagrams using Stereonet. Stream-course data for linear segments exhibit three dominant trends 1) 015°-195° +/- 15°, 2) 095°-275° +/- 15°, and 3) 155°-335° +/- 15° and one minor trend (130°-310° +/- 10°) above background scatter (Figure 8). The northward trend of the petals on the rose diagrams reflects the northerly flow of Rocky Creek. Joint orientation data for 321 joints exhibit four dominant trends 1) 015°-195° +/- 15°, the NE-SW set 2) 095°-275° +/- 15°, the E-W set 3) 130°-310° +/- 10°, and 4) 155°-335° +/- 10°, the NW-SE set (Figure 7). The first two sets are more dominant and occurred twice as frequently as the latter two sets. The stream data show a stronger northwest-to-southeast trend (155°-335° +/- 15°), although the associated joints are not well exposed in outcrop. Because the outcrops trend northwest for over 300 m, these joints (155°-335° +/- 15°; 130°-310° +/- 10°) intersect the outcrops at oblique angles. Thus, the above joint sets are dif-

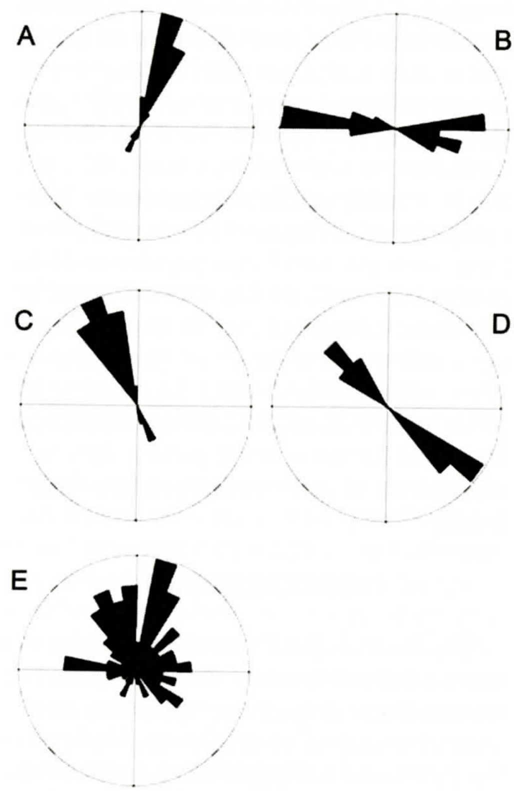

Figure 8. Equal-area rose diagrams of stream segments measured at Broxton Rocks. A: 015°-195° +/- 15°, 21 segments (circle- 38%); B: 095°-275° +/- 15°, 21 segments (24%); C: 155°-335° +/- 10°, 20 segments (30%); D: 130°-310° +/- 10°, 14 segments (29%); E: 101 stream segments of Rocky Creek downstream of Rock Falls.

ficult to identify and measure through a significant portion of the large outcrop (Figure 6). Joints corresponding to the other three trends at other angles are more visible in outcrop and are better represented in the data. Additional descriptions of individual joints are available in the appendix of Davis (2004).

Age relationships were determined in the field using 40 joints ranging from 10 cm to 40 m in length. Based on the joints measured on the topographic surface of the exposures (n=45), the E-W set is older than the N-S set (Figure 4). Of the joints exposed on vertical faces (n=276), the NW-SE set is older than the NE-SW. Although the NW set (155°-335°) is not observed frequently in the outcrop, the NW set occurs frequently in the stream-course data. We were unable to determine the relative ages of all of the joint sets to one another due to a lack of sufficient field data.

DISCUSSION

The orthogonal intersection of the joint sets produces the rectilinear drainage pattern through which Rocky Creek flows as it makes its way northward through the Broxton Rocks Preserve toward the Ocmulgee River (Figures 5,6). McCulloh (2003) proposed that rectilinear stream patterns in Louisiana might be controlled by underlying geologic features such as faults and joints. Because most of Louisiana is covered by unconsolidated alluvium and other sediment that frequently does not exhibit joints, establishing a relationship between drainage patterns and underlying geology is problematic (McCulloh, 2003). The Atlantic Coastal Plain of Georgia and South Carolina is geologically similar to the area McCulloh (2003) studied. At Broxton Rocks, however, joint sets can be identified and measured. Furthermore, the rectilinear pattern of Rocky Creek is visually obvious (Figure 5). Even though the Coastal Plain lies on a passive margin, tectonic stresses do exist in the region. Clearly, adequate stresses exist to initiate and propagate numerous joints throughout the southern Atlantic Coastal Plain.

Stresses affecting the Coastal Plain of Georgia and South Carolina occur at a variety of scales and magnitudes. Engelder (1993) proposed that the Mid-Plate of the North American Plate, an area encompassing the Great Plains to the Atlantic coastline, is affected by a NE-SW compression. Lord (1992) indicated through tectonic models and numerous field measurements that the eastern U.S. is under a regional NE-SW compression along with a more local NW-SE compression in Georgia and Alabama. Talwani (1990) determined a maximum horizontal stress ($\underline{S}_H$) with a direction of 63° from focal mechanisms near Charleston, South Carolina. Another cause of regional stress may be the slight velocity deviations of the North American and Caribbean Plates and/or differences in velocity within the continental and oceanic components of the North American

Plate (M.J. Bartholomew, personal communication, 2003).

Another origin of stress affecting the region results from the dissolution of carbonate in Oligocene and Eocene limestone units in north-central Florida. Crustal unloading at a rate of 1.2 x 10^6 m^3/yr may have caused at least 36 m of isostatic uplift in the shallow crust since the Pleistocene (Opdyke and others, 1984). The lithostatic pressure released from the removal of overlying strata may have contributed sufficient stress for rocks to fracture. However, localized stress caused from unloading and pressure release will usually not form joints with preferred orientations (M.J. Bartholomew, personal communication, 2003). Such local, non-directional stress will propagate joints in all directions, resulting in even petals in all directions on the rose diagrams. Therefore, preferred joint orientations result from directed stresses throughout the region, especially because these trends are common over a large geographic area.

Regardless of the possible origins of stress, Bartholomew and others (1997) identified the deformational sequence that produced the joints in the southern Atlantic Coastal Plain. According to those authors, the sequence from oldest to youngest, is as follows: a NE-SW extension, N-S extension, E-W extension, and NW-SE extension. This sequence of extension events correlates well with the age relationships of joints established from Broxton Rocks. The last extension event is compatible with the NE-SW compression of the modern stress field indicated previously by Engelder (1993) and Lord (1992). The N-S extension and frequently an E-W compression have dominated the area since the Alleghanian Orogeny (Bartholomew and others, 1997). However, stress fields are not permanent features in a region because tectonics change over time; the modern stress field in the southern Atlantic Coastal Plain has existed since the Pliocene (Bartholomew and others, 1997).

Identifying regional tectonic stresses is problematic, and associating a specific stress field with a particular joint set is nearly impossible. According to Davis (1984), many factors contribute to the elusive formation of a joint. First, establishing the time of formation of specific joints or sets of joints and knowing exactly when they formed relative to a single deformational event is potentially complex. Second, joints may be activated and reactivated during single or multiple deformational events. Third, many different physical processes produce joints, and it is not always possible to distinguish which one explains a specific joint set. Therefore, it is critical that the researcher does not correlate a joint set with a specific tectonic stress without understanding the complete tectonic history of an area. Still, according to Davis and Reynolds (1996, p.268) "there is always plenty of room for independent, creative inquiry."

CONCLUSIONS

The Broxton Rocks Preserve contains Miocene sandstone outcrops of the Altamaha Formation. These sinuous outcrops bear numerous vertical and sub-vertical joint sets within them. Four joint orientations exist at Broxton Rocks: two major sets, NE-SW (015°-195°) and the E-W set (095°-275°) and two minor sets, the NW-SE set (155°-335°) another northwesterly set (130°-310° +/- 10°). This latter set is visible in both the joint and stream data. A weak N-S (355°-175°) exists primarily in the large outcrop-dissecting fractures on the topographic surface. Age relationships based joint intersections show the E-W set is older than the N-S set, and the NW-SE set is older than the NE-SW set. Due to the lack of collected age relationship data, a complete chronology of relative ages was not undertaken. Similar orientations and relative age relationships of joint sets have been observed in other formations of comparable ages throughout the southern Atlantic Coastal Plain and in northern Louisiana. Although the modern stress field is understood in Georgia and South Carolina, it is difficult to extrapolate the stress field to encompass all of the Atlantic and Gulf Coastal Plains. However, consistent orientations of joint sets at Broxton Rocks suggest these features were caused by known regional tectonic stresses with preferred directions. The two orthogonal joint sets at Broxton Rocks influence the course of Rocky Creek, which flows in a rectilinear pattern through a section of the property. Thus, Broxton Rocks is a structurally controlled landform on a passive continental margin. The Broxton Rocks Preserve also contains numerous species of flora and fauna, some of which are rare to the Coastal Plain. With geological and biological attributes that are unique to southern Georgia, Broxton Rocks will merit continued conservation for the enjoyment and education of future generations.

ACKNOWLEDGEMENTS

Thanks are expressed to Professor Frankie Snow, Natural Science and Mathematics Division at South Georgia College, for introducing us to the natural history of the property and providing biodiversity information about the Broxton Rocks Preserve. The Nature Conservancy, along with Mr. Snow, deserves our thanks for allowing permission to conduct fieldwork on the property. Assistance from Mervin J. Bartholomew, University of Memphis, was critical in providing detailed insight into the tectonic history and joint development in the region. We are also grateful to Charles H. Trupe, Dallas D. Rhodes, and Mervin J. Bartholomew for thorough review of this manuscript. We thank Richard P. McCulloh and Carl R. Froede, reviewers for *Southeastern Geology*, for constructive comments resulting in a better manuscript, and Duncan Heron, editor, for his assistance in the final steps of the manuscript. Thanks are also due to Michael Robinson, Sunni Holland, Susan Howell, Martin Jones, Matthew Hampton, and Lindsey Kraatz for their contributions. Special thanks to the Department of Geology and Geography and the Academic Excellence Committee of the Allen E. Paulson College of Science and Technology at Georgia Southern University for funding the majority of this project.

REFERENCES CITED

Bartholomew, M.J., Rich, F. J., Lewis, S.E., and Brodie, B.M., 1997, Neogene/Quaternary deformation sequence, Atlantic Coastal Plain: Geological Society of America, Southeastern Section, Abstracts with Programs, v. 29, no. 3, p. 4

Bartholomew, M.J., Rich, F.J., Whitaker, A.E., Lewis, S.E., Brodie, B.M., and Hill, A.A., 2000, Neotectonic features of the Lower Coastal Plain of Georgia and South Carolina: *in*, Abate, C, and Maybin, B. (eds.), A Compendium of Field Trips (#3) of South Carolina Geology with Emphasis on the Charleston, South Carolina, Area: South Carolina Department of Natural Resources, Geological Survey, p. 19 - 30.

Bartholomew, M.J., personal communication. Memphis, TN, March 13, 2003.

Blanchard, John S., Snipes, David S., Hodges, Rex A., Bartholomew, Mervin J., Temples, Thomas J., 1997, Extensional Joints in the Tobacco Road and Altamaha Formations at the Savannah River Site: Geological Society of America, Southeastern Section, Abstracts with Programs, v. 29, no. 3, p. 5.

Dall, W.H. and Harris, G.D., 1892, Correlation papers Neocene: U.S. Geological Survey Bulletin 84, p. 107-111.

Davis, G.H., 1984, Structural geology of rocks and regions: New York City, New York, John Wiley & Sons, Inc, p. 325-353.

Davis, G.H. and Reynolds, S.J., 1996, Structural Geology of Rocks and Regions: New York City, New York, John Wiley & Sons, Inc, 776 p.

Davis, L.A., 2004, An Investigation of Fracture Sets and Rare Biota at the Broxton Rocks Preserve, Altamaha Formation, Coffee County, Georgia: unpublished Bachelor's thesis, Georgia Southern University Department of Geology and Geography, p. 33.

Dutton, C.E., 1889, The Charleston Earthquake of August 31, 1886: U.S. Geological Survey Annual Report, 1887-1888, p. 203-528.

Engelder, T., 1993, Stress Regimes in the Lithosphere: Princeton, New Jersey, Princeton University Press, p. 337-383.

Freeman, T., 1999, Procedures in Field Geology: Malden, Massachusetts, Blackwell Science, Inc., p. 18-20.

Huddlestun, P.F., 1988, A Revision of Lithostratigraphic Units of the Coastal Plain of Georgia, The Miocene Through Holocene: Georgia Geological Survey Bulletin 104, 162 p.

Lord, K.M., 1992, A binary lithospheric stress field model for the Eastern U.S.: Seismological Society of America, Eastern Section, v. 63, no. 4, p. 610.

McCulloh, R.P., 2003, The stream net as an indicator of cryptic systematic fracturing in Louisiana: Southeastern Geology, v. 42, no. 1, p. 1-17.

Opdyke, N.D., Spangler, D.P., Smith, D.L., Jones, D.S., and Lindquist, R.C., 1984, Origin of the epeirogenic uplift of the Pliocene-Pleistocene beach ridges in Florida and development of the Florida karst: Geology, v. 12, p. 226-228.

Snow, F., 1994, Broxton Rocks Preserve Design: Unpublished report submitted to The Nature Conservancy, South Georgia College, Douglas, Georgia, 21 p.

Snow, F., personal communication. Douglas, GA, March

22, 2003.

Talwani, P. and Marple, R.T., 1997, Evidence of neotectonic activity in the South Carolina Coastal Plain: Proceedings from the 30th International Geological Congress, v. 5, p. 49-61.

Talwani, P., 1990, Neotectonics in the Southeastern United States with emphasis on the Charleston, South Carolina, area, Reviews in Engineering Geology, v. 8, p. 111-129.

Washington, P.A., 1998, Regional joint patterns in NW Louisiana; evidence for two-phases of compressional tectonics: AAPG Bulletin, v. 82, no. 9, p. 1795.

Washington, P.A., 2003, Regional joint patterns in Eocene strata of northern Louisiana: correlations with neotectonic features: Geological Society of America, Southeastern Section, Abstracts with Programs, v. 35, no. 1, p. 21.

SOUTHEASTERN GEOLOGY
V. 44, No. 1, October 2005, p. 37-44

DISTRIBUTION OF HIGH-LEVEL ALLUVIAL DEPOSITS IN THE VALLEY AND RIDGE OF POLK COUNTY, SOUTHEASTERN TENNESSEE: IMPLICATIONS FOR RIVER HISTORY AND DRAINAGE EVOLUTION

HUGH H. MILLS

DAVID N. SUMNERS

EVAN A. HART

PETER LI

Department of Earth Sciences
Tennessee Technological University
Cookeville, TN 38505
hmills@tntech.edu

ABSTRACT

Surficial mapping based on digital soil maps along the Hiwassee and Ocoee Rivers in western Polk County, Tennessee, shows almost 100 square kilometers of alluvium. By far the most extensive is high-level alluvium resting on carbonate bedrock, mainly on the Knox Group. This old alluvium covers rolling topography at elevations of roughly 15 m or greater above the modern river level (ARL), extending to 80 m ARL locally. It is highly weathered, with B horizons having clay percentages exceeding 50 percent and Munsell hues of typically 2.5YR. Sandstone clasts, where present, generally are decomposed. Deposits lower than 15 m ARL occur on floodplains and low terraces are much less weathered, with clay percentages less than 30 and colors no redder than 7.5YR. Pebbles and cobbles of vein quartz attest to the origin of most alluvium in the Blue Ridge province. Such clasts become less common with increasing height ARL, and at the highest levels regolith consists of scattered quartz clasts mixed with carbonate residuum. Alluvial deposits generally occur within 4 km of the main rivers. An exception is a band of high-level alluvium extending from the Ocoee south-southwesterly to the Conasauga River near the Tennessee-Georgia border. This band crosses a prominent divide between the Tennessee and Coosa River basins where only small, local streams flow today. Its presence suggests either that the Conasauga, currently a tributary to the Coosa, once flowed north to the Tennessee River, or else that the Ocoee, now a tributary of the Tennessee, once flowed south to the Coosa.

INTRODUCTION

Alluvial deposits are widespread in the Valley and Ridge physiographic province where they are preferentially preserved over carbonate bedrock owing to the dominance of solution and internal drainage on this rock type (Houser, 1981, Fig. 21-22; Bell, 1986). Since some of these alluvial deposits correlate well with soil series, digital soil maps can readily be utilized to make maps of the deposits. For our study we selected Polk County, Tennessee (Fig. 1), which was known to have abundant alluvial deposits and for which a digitized Natural Resources Conservation Service (NRCS) soil map is available (Newton and Moffitt, 2001). The study area, western Polk County, lies in the Valley and Ridge and Blue Ridge physiographic provinces, the boundary between the two being the contact between Precambrian and Cambrian rocks. The main streams in the area are the Hiwassee River, the Ocoee River, and the Conasauga River (Fig. 2). All drain the Blue Ridge province and carry abundant pebbles and cobbles of vein quartz. The Ocoee joins the Hiwassee, which then drains to the Tennessee River to

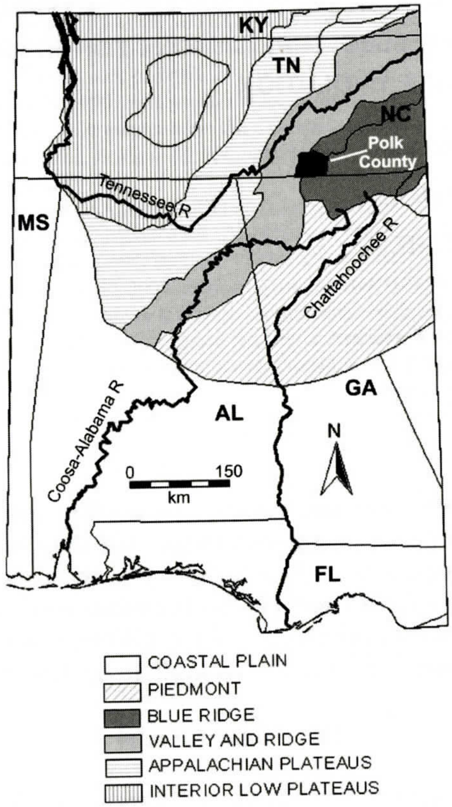

Figure 1. Location map for study area in Polk County, Tennessee. Note Tennessee and Coosa Rivers. State symbols: AL = Alabama, FL = Florida, GA = Georgia, KY = Kentucky, MS = Mississippi, NC = North Carolina, TN = Tennessee.

the west. The Conasauga, in contrast, flows southwest and joins the Coosa River which then flows to the Gulf.

The purposes of this study were: 1) to measure the degree of weathering of the alluvium as a function of height above modern river level (ARL) to see whether we could discern a change in river regime through time, and 2) to determine the spatial distribution of the alluvium in order to make inferences concerning possible drainage evolution.

SOIL MAPS AND ALLUVIAL DEPOSITS OF WESTERN POLK COUNTY

Intensive study of surficial deposits in the Oswald Dome and Benton quadrangles in Polk County (Mills, unpub. data) showed very good correlations between mapped soil series and alluvial deposits. For example, flood plains on major streams were mapped by the NRCS as Toccoa loam, low terraces on the same streams as Sequatchie Silt Loam, and high terraces largely as Waynesboro series. Based on this preliminary study, we made the assumption that these correlations existed elsewhere in Polk County and used them to map the alluvium.

As Figure 2 shows, the extent of alluvial deposits amounts to almost 100 km^2 in western Polk County. Further, as Figure 2 indicates, most of the alluvium stands high ARL. Such deposits are best referred to as "high-level alluvium" rather than terraces, for their surfaces are rolling rather than flat like terraces, presumably owing to karstification of the underlying carbonate bedrock. Approximately 85 percent of the mapped alluvium is of the high-level type, with floodplains and low terraces accounting for only a small part of the total area.

The high-level alluvium differs distinctly from that on floodplains and low terraces. First, the greater height ARL of this alluvium suggests that it is substantially older than deposits on floodplains and low terraces. Whereas low terraces are no higher than 15 m ARL, the high alluvium exceeds 80 m ARL locally. Based on a regional erosion rate of about 30 m/my (Hack, 1980; Matmon and others, 2003), the 80-m height represents an age of 2.67 Ma for high alluvium. However, since deposits on carbonates can probably be let down great distances vertically without being eroded away, the age could probably exceed Pliocene.

The break between the low terraces and the high alluvium, which occurs at 10-15 ARL, appears distinctive. The low terraces are flat, whereas the topography of the high alluvium is rolling. Our field data also indicate a distinctive weathering difference between high alluvium and low terraces. Above 10-15 m ARL the de-

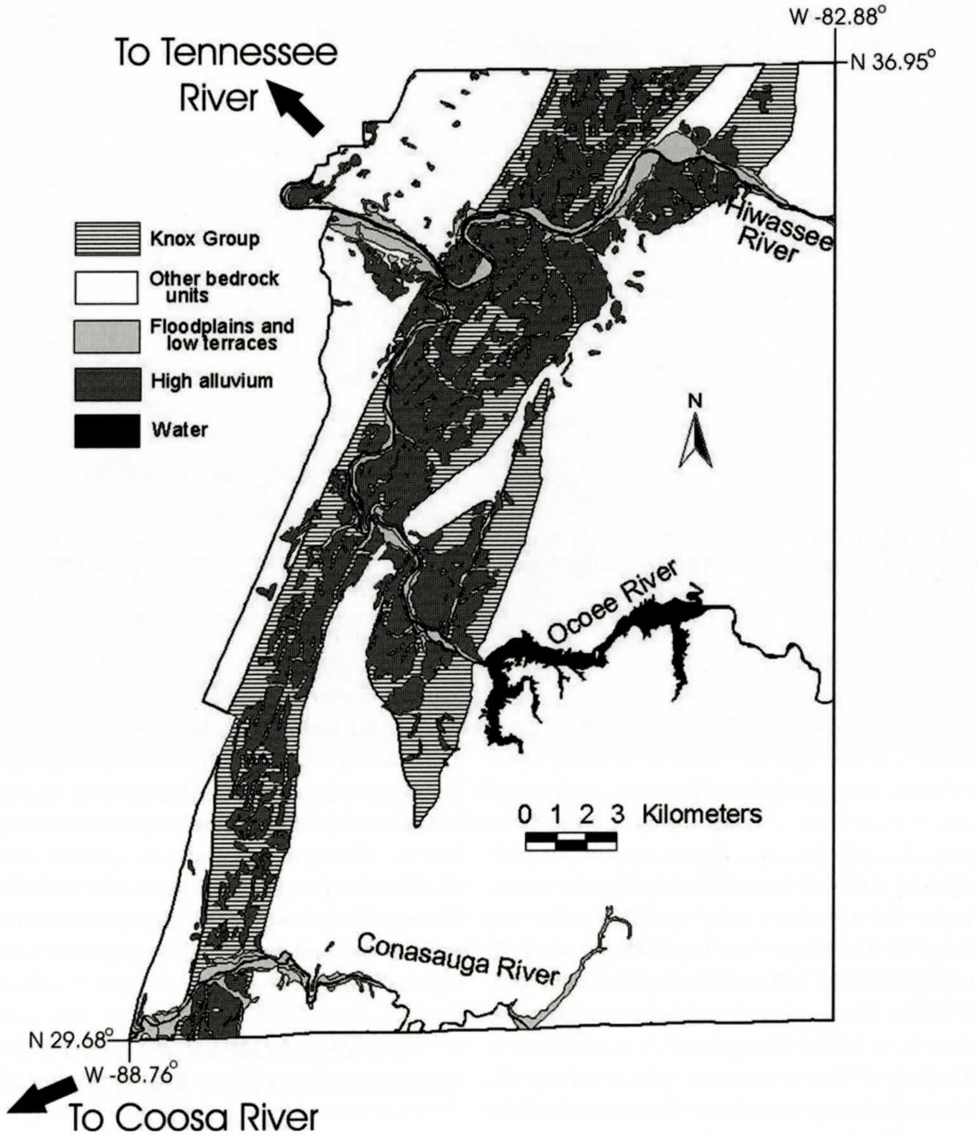

Figure 2. Map of alluvial deposits and their relationship to the Knox Group outcrop in western Polk County. Map of Knox Group from Hardeman,1966. Deposits and geology outside of the county boundary are not shown.

posits are red and clayey, whereas below this level they are brown and loamy. As Figure 3 shows, typically the B horizons of high-level alluvium contains 50 percent or greater clay, vs. only 30 percent for B horizons of the low terraces. In addition, the higher alluvium has a Munsell hue of 5.0YR or 2.5YR, whereas the younger ranges from 10YR to 7.5YR.

Figure 4 shows the elevation ARL frequency distribution for a large part of the alluvial surfaces shown in Figure 2. This distribution was determined by overlaying the digital soil map onto a 30-m DEM of the Oswald Dome and Benton 7.5-minute quadrangles. Points with slopes greater than 3° were excluded in order to decrease the influence of terrace risers and erosional slopes on the distribution. The shape of the frequency distribution suggests inferences

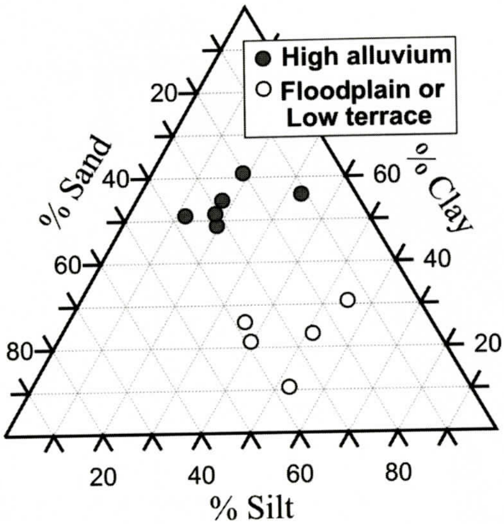

Figure 3. Ternary diagram contrasting particle-size distribution of low and high alluvial deposits.

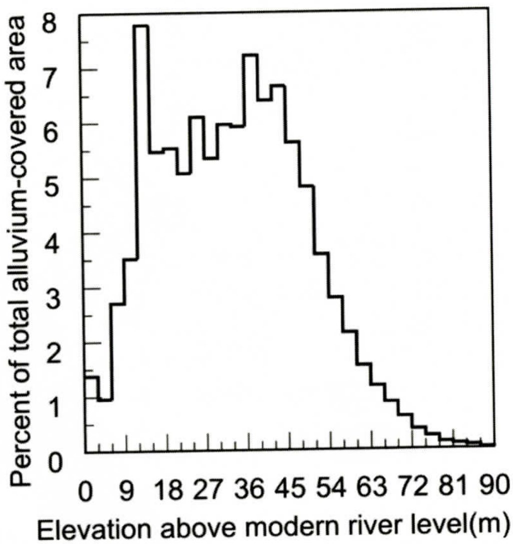

Figure 4. Histogram showing frequency distribution of elevation ARL of alluvium-covered surfaces in northwestern Polk County, Tennessee.

about long-term regime changes of the Hiwassee and Ocoee. In contrast to the New River of southwestern Virginia (Mills, 1986, Mills and Wagner, 1985), the distribution is much more uniform, lacking the pronounced modes and gaps between the modes shown by the New River. As such modes and gaps may indicate alternating intervals of equilibrium and downcutting, their absence may indicate that the Hiwassee and Ocoee did not undergo such alternations. Note, however, that there is no low-elevation mode such as might result from the presence of broad floodplains, as is seen for the New River. The absence of such a low-elevation mode in the frequency distribution could indicate that recent downcutting has stranded former floodplains as present-day low terraces.

Another difference between high and low alluvium concerns the frequency, composition, and condition of pebbles and cobbles. Large, well rounded pebbles and cobbles are common in the higher deposits, but rare in the lower ones (Figure 5). This difference probably stems from the fact that younger alluvium commonly is covered by overbank deposits. Presumably the old alluvium was once so covered, but these deposits have been stripped by erosion, exposing the gravelly channel deposits beneath. Clasts of sandstone in high-level alluvium commonly are weathered and friable. At higher levels, most clasts are quartz, as sandstone has disintegrated and is no longer present. With increasing height ARL, clasts become more scarce. At still higher levels, "alluvium" consists of scattered cobbles of vein quartz mixed with carbonate residuum. Ultimately, of course, all the quartz is weathered away and only residuum underlies the highest hilltops.

POSSIBLE IMPLICATIONS FOR STREAM HISTORY AND DRAINAGE EVOLUTION

The huge area of high-level alluvial deposits relative to that of floodplains and low terraces is puzzling. One might expect high-level deposits to be less plentiful than low-level ones, as the former have been exposed to erosion much longer that the latter. This apparent conundrum might have several possible explanations, including: 1) Earlier in the Cenozoic, tectonic or climatic conditions favored the production of wide floodplains. Since that time, downcutting has been the dominant stream regime, so that such floodplains are no longer produced, and

Figure 5. Photograph of gravel-rich high-level alluvial deposit. Pencil is 15 cm long. Clasts are composed mainly of vein quartz, quartzite, and sandstone.

the high-level deposits we see today are the remains of these broad floodplains; 2) There never were floodplains as broad as the area covered by today's high-level deposits. Instead, the widespread occurrence of high-level deposits results from the great age span over which they were laid down. Over millions of years the major streams have moved their locations extensively, gradually covering with alluvium the wide area we see today. Thanks to the preserving action of the widespread carbonate bedrock, these deposits still exist, albeit in a highly weathered state.

Another question related to the widespread nature of the high-level deposits is why they are almost completely confined to the Knox Group (Fig. 2). One possible answer is that the Knox is highly erodible, as indicated by the low relief and slope characteristic of Knox Group outcrops throughout the Tennessee Valley and Ridge (Mills, 2003). For this reason the Knox underlies valleys and is likely to be occupied by a river and thus eventually covered by floodplains and terraces. An alternative answer, however, is that because transported regolith tends to be preserved over carbonate bedrock, we are simply looking at a case of selective preservation. That is, the course of the rivers may have shifted widely through time, occupying other rock units than the Knox, but only deposits on the Knox (the dominant carbonate unit in western Polk County) have survived. In other words, the total area once covered with river deposits may actually once have been somewhat larger than what we see today.

Alluvial deposits occur chiefly within 4 km of the main rivers, suggesting that in general the ancient river courses were not greatly different from present courses. A significant exception, however, is a band of old alluvium extending about 15 km from the Ocoee River south-southwesterly to the Conasauga River near the Ten-

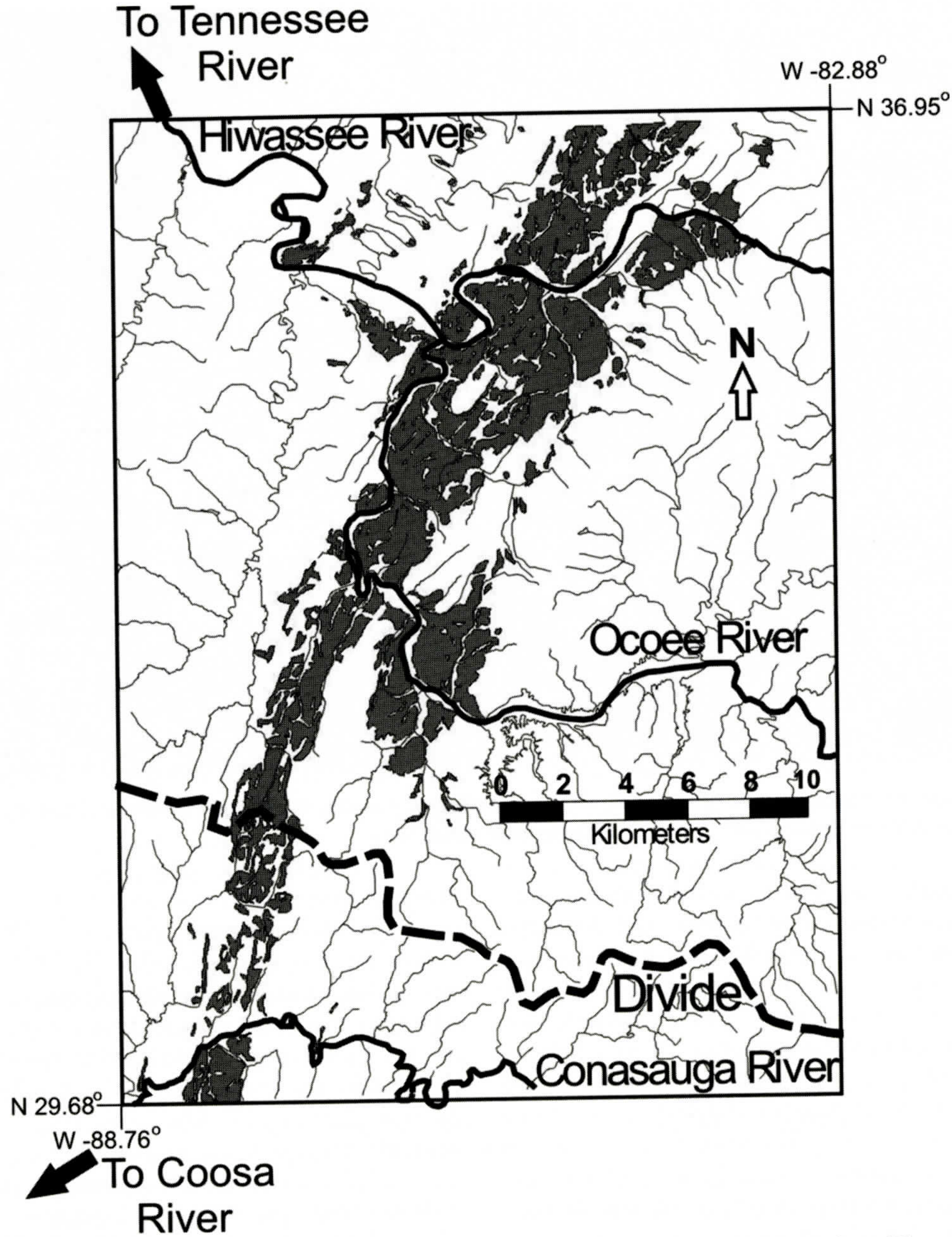

Figure 6. High-level alluvial deposits (shaded pattern) in relation to stream network and the major divide between the Coosa River drainage and the Tennessee River drainage in western Polk County.

nessee-Georgia border (Figures 2 and 6). This band of alluvium crosses a major divide between the Gulf Coast drainage and the Tennessee River drainage, where only small local streams flow today. Field inspection shows that these old alluvial deposits contain cobbles of vein quartz, demonstrating that they could not have originated from local bedrock but must have come from the Blue Ridge province. The presence of a large stream is thereby indicated, even though many of the deposits subsequently may have been reworked by small streams or colluviation.

The location of the band of alluvium suggests that at one time either the Conasauga River flowed to the Ocoee River and thence to the Tennessee River, or the Ocoee flowed to the Conasauga and thence to the Coosa. Although the linear band of alluvium may owe its shape to selective preservation on the Knox, that effect alone would not account for the presence of quartz cobbles along the band. This presence requires that rivers of some kind flowed from the Blue Ridge to this location, even though the geometry of the river courses may have been quite different from that suggested by this linear corridor.

If we assume that the deposits between the Ocoee and the Conasauga really do represent a former stream course, just what was flowing where? Did the Ocoee River once flow to the Conasauga or did the Conasauga flow to the Ocoee and thence to the Tennessee? Evidence that bears on this question is sparse. Certainly the steeper mean gradient of a course directly to the Gulf as opposed to the much longer course to the Gulf via the Tennessee would favor migration of the divide northward toward the Tennessee River. On the other hand, at the location where the Ocoee and Conasauga are closest together, the Conasauga is actually about 10 m higher than the Ocoee, which would favor migration southward. To be sure, this elevation difference is a small one, so that at this time there simply is insufficient evidence to speculate on the paleodrainge.

CONCLUSIONS

Alluvial deposits are widespread in the Valley and Ridge and provide evidence for the history of stream regime and drainage evolution. In particular, the extent of old, high-level deposits overlying carbonate bedrock is impressive. It is probable that in this province there are a number of strike valleys such as the one described herein, occupied today only by small local streams, which once were occupied by large rivers. Remnant quartz-bearing alluvium testifies to the presence of such rivers. The rapidly increasing number of digital NRCS county soil maps promises to greatly increase the rate at which such alluvium can be mapped and should substantially increase our understanding of long-term changes in stream regimes and drainage systems in this physiographic province.

Although the drainage history and evolution in the present study area cannot yet be definitively delineated, the potential of the application of digital soil maps seems apparent. One strength of this approach is that it offers alluvial evidence. Many speculations concerning major changes in Appalachian drainage have been based on morphology alone, with no or little surviving alluvium to provide supporting evidence (e.g., development of wind gaps in the Blue Ridge of Virginia [Thornbury, 1965, p. 102]; retreat of the Blue Ridge escarpment [Thornbury, 1965, p. 104-196]; and evolution of the course of the Tennessee River [Thornbury, 1965, p. 124-126]).

ACKNOWLEDGEMENT

We thank the US Geological Survey NCG-MP Appalachian Blue Ridge Project for field support, and Scott Southworth for assistance.

REFERENCES CITED

Bell, A. M., 1986, Morphology and stratigraphy of terraces in the upper Shenandoah Valley, Virginia [MS thesis]: West Virginia University, Morgantown, 160 p.

Hack, J. T., 1980, Rock control and tectonism – their importance in shaping the Appalachian Highlands: U.S. Geological Survey Professional Paper 1126-B, p. B1-B17.

Hardeman, W. D., 1966, Geologic Map of Tennessee. Tennessee Division of Geology Map, Nashville, TN, 4 sheets, scale 1:250,000.

Houser, B., 1981, Erosional history of the New River, southern Appalachians, Virginia: U.S. Geological Survey Open-file Report 81-0771, 226 p.

Matmon, A., Bierman, P., Larsen, J., Southworth, S., Pavich, M., and Caffee, M., 2003, Temporally and spatially uniform rates of erosion in the southern Appalachian Mountains: Geology, v. 31, p. 155-158.

Mills, H. H., 1986, Possible differential uplift of New River terraces in southwestern Virginia: Neotectonics, v. 1, p. 75-86.

Mills, H. H., 2003, Inferring erosional resistance of bedrock units in the east Tennessee mountains from digital elevation data: Geomorphology, v. 55, p. 263-281.

Mills, H. H., and Wagner, J. R., 1985, Long-term change in regime of New River indicated by vertical variation in extent and weathering intensity of alluvium: Journal of

Geology, v. 93, p. 131-142.
Newton, D. L., and Moffitt, W. C., 2001, Soil Survey of Polk County, Tennessee: Natural Resources Conservation Service, 298 p.
Thornbury, W. D., 1965, Regional geomorphology of the United States: New York, Wiley, 609 p.

SOUTHEASTERN GEOLOGY
V. 44, No. 1, October 2005, p. 45-51

The Impact of Hurricane Georges (September 28, 1998) Across Dauphin Island, Alabama

Carl R. Froede Jr.

United States Environmental Protection Agency
Region 4
61 Forsyth Street
Atlanta, GA 30303-8960

ABSTRACT

On the morning of September 28, 1998, Hurricane Georges (a Category 2 hurricane on the *Saffir-Simpson* scale) made landfall between the towns of Ocean Springs and Biloxi, Mississippi. Passing well to the west of Dauphin Island, the storm still impacted the island with wind speeds up to 129 km/hr (a Category 1 hurricane on the *Saffir-Simpson* scale). This resulted in substantial changes along the island's gulf side. The eastern end of the island experienced a storm surge along with accompanying storm waves that easily overtopped the swash zone berm crest. Storm waves washed tens of meters landward and flattened the beach profile. Much of the western end of the island was completely overwashed by storm waves. As of early 2005, natural shoreline processes have not restored the pre-storm beach profile or returned the swash zone to its former position. Tropical storms and hurricanes that impact the island reveal its vulnerability and dependence on regular sand nourishment. Hurricane Georges exposed the fragile nature and precarious setting of Dauphin Island in the Gulf of Mexico.

INTRODUCTION

Dauphin Island is a 22.5-km long micro-tidal barrier island located approximately eight kilometers offshore from the southwestern end of Alabama (Figure 1). It serves as an excellent locale from which to study a variety of coastal processes under varying conditions. While the island is adjacent to the Mobile Bay ebb-tidal delta it still requires periodic sand nourishment in order to retain its general shape and size. Tropical storms and hurricanes tend to modify the island in dramatic ways (e.g., Nummedal and others, 1980; Penland and others, 1980; Schramm and others, 1980; U.S. Army Corps of Engineers, 1981; Froede, 1998, 2005). Hurricane Georges exposed the fragile nature and precarious setting of Dauphin Island in the Gulf of Mexico.

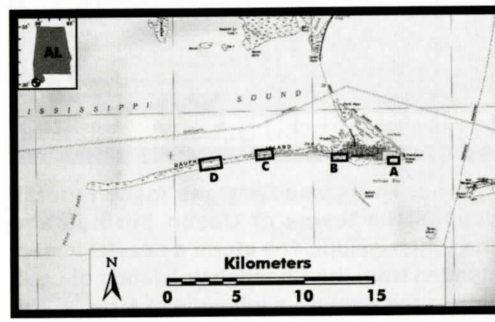

Figure 1. Dauphin Island, Alabama. The island is eight kilometers offshore from the southwestern end of Alabama. It is approximately 22.5 km in length and comprised of an eastern barrier island and western sand ridge. The various boxes across the island refer to areas discussed and photographed within the context of this paper. Map constructed from the U.S. Geological Survey, Biloxi: MISS.-ALA.-LA., 1:100,000 scale topographic map.

HURRICANE GEORGES

Tropical Depression Georges formed off the western coast of Africa on September 15, 1998, and reached hurricane status on September 18th (Guiney, 1999). The storm entered the Gulf of Mexico as a Category 2 hurricane (*Saffir-Simpson* scale) on September 26, 1998.

On the morning of September 28, 1998, Hur-

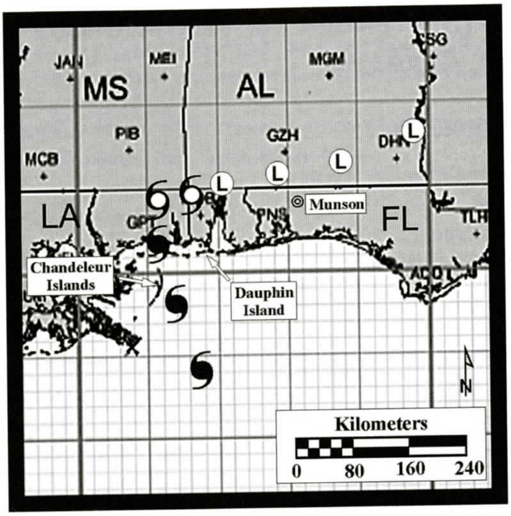

Figure 2. Hurricane Georges made landfall between the towns of Ocean Springs and Biloxi, Mississippi. The storm's coastal impact extended from the Chandeleur Islands of Louisiana to the western panhandle of Florida. The hurricane quickly diminished to a tropical storm and then a tropical depression once it moved inland. It dropped considerable precipitation as it moved east-northeast across south Mississippi and southern Alabama. The highest recorded rainfall occurred at Munson, Florida. Storm data from U.S. Army Corps of Engineers (1999) covering a period from September 27 to October 1, 1998.

ricane Georges slowed as it made landfall between the towns of Ocean Springs and Biloxi, Mississippi (Figure 2). Storm winds measured at 170 km/hr made it a Category 2 hurricane on the *Saffir-Simpson* scale. It created an exceptionally elevated tidal surge along the central gulf coast ranging from 3.3 m in eastern Mississippi to 2.3 m in the western panhandle of Florida (U.S. Army Corps of Engineers, 1999). These water levels were further increased with the addition of storm waves. The resulting coastal damage extended from the Louisiana Chandeleur Islands to the panhandle of Florida (Turnipseed and others, 1998; Guiney, 1999; Stone and others, 1999; Liebens, 2000).

Once inland, the slow moving tropical depression created significant flooding along many of the creeks and streams in southern Alabama and along the Florida panhandle. Turnipseed and others (1998) reported rainfall amounts generally between 38.1 to 63.5 cm with the highest level (i.e., 97.68 cm) recorded at Munson, Florida.

Table 1. Hurricane Georges had considerable impact across the island as a Category 1 hurricane (*Saffir-Simpson* scale). Data from various NOAA and USGS sources (Turnipseed and others, 1998; Guiney, 1999; NCDC-NOAA, 1999)

Hurricane Georges's Impact to Dauphin Island [exception noted in brackets]	
Wind Speed (peak gusts)	128.75 km/hr
Storm Waves (Alabama coast)	7.62 m
Storm Surge (above mean sea level)	1.61 m
Barometric Storm Pressure [measured in Biloxi, MS area]	[960 mb]
Rainfall (September 28th to 30th total range estimates)	30.3 to 33.0 cm

SEDIMENT TRANSPORT ALONG THE ISLAND

Published studies undertaken during periods of fair-weather have documented the changing foreshore swash-zone and lower beach profiles (Hardin and others, 1976; Smith and Parker, 1990). Sediment transport and the associated accretion or erosion of the gulf-facing shoreline of the island has also been investigated (Douglass, 1994; Douglass 2001; Sanchez and Douglass, 1994). This recent work determined that westward-directed littoral drift is the dominant means by which quartz sand and other clastic sediments are transported along the Gulf of Mexico side of the island. Additionally, a seasonal cycle of offshore and onshore sand transport was also noted for certain shoreline areas. However, deviations to these typical sedimentary patterns were likewise documented (Sanchez and Douglass, 1994). Hence, the erosion, transport, and deposition of sand along the shoreline varies across the island by locale and rate.

CHANGES INDUCED BY HURRICANE GEORGES

Hurricane Georges impacted Dauphin Island

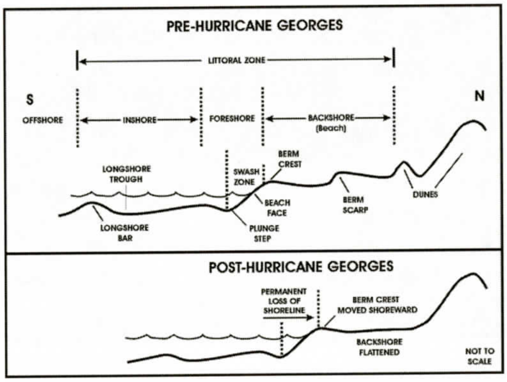

Figure 3. Generalized pre- and post-storm beach profiles for the eastern portion of Dauphin Island. The backshore profile shortens along the gulf side of the island moving westward along the island's shoreline. In the area of the picnic pavilions, the storm surge can easily extend across the truncated beach to the base of the large upland dune ridge. Modified from Smith and Parker (1990, Figure 11).

with wind speeds up to 129 km/hr (a Category 1 hurricane on the *Saffir-Simpson* scale). However, erosional damage to the island was largely from surging tide and storm waves [Table 1]. The shoreline and beach profile for many areas along the gulf side of the island were significantly altered (Figure 3). The landward migration of the swash zone at several localities moved shoreward from three to 10 meters and storm waves washed inland tens of meters. In other areas storm water was powerful enough to completely overwashed the island. Some of the beaches experienced an accretion of sand to the existing shoreline actually expanding the resulting flattened and featureless backshore area.

Eastern End Of Dauphin Island

Along the eastern end of Dauphin Island, the combination of a rising storm surge coupled with substantial storm waves allowed breakers to wash ashore for tens of meters beyond the normal swash zone. Rising storm water easily overtopped the swash zone berm crest and surged across the gulf-facing side of the island. Small-scale vegetation was removed or buried by sand that advanced with the rising storm water and waves. The foreshore swash zone migrated inland on average between three and four meters. Both the swash zone and beach profile were transformed from their pre-hurricane position and shape (Figures 4A and 4B).

Figures 4A and 4B. Southeastern end of Dauphin Island. Photograph (A) was taken March 1998, and photograph (B) was taken December 1998. Note the arrow that points to the same pine tree. The combination of storm surge and large waves allowed water to overflow across the backshore portion of the island. Sand was washed shoreward filling in low-lying areas and flattening preexisting berm ridges. Small-scale vegetation was either washed away or buried. As of early 2005, this portion of the island has not returned to its pre-Hurricane Georges profile or its former swash zone position. This location is in Figure 1, Box A.

The Dauphin Island Pier And Picnic Area

In the area to the immediate east of the pier, storm water surged across the backshore. This flattened the preexisting surface features resulting in the development of a broad beach which extended landward to one of the larger dunes in the backshore area. An area of exposed paleosol

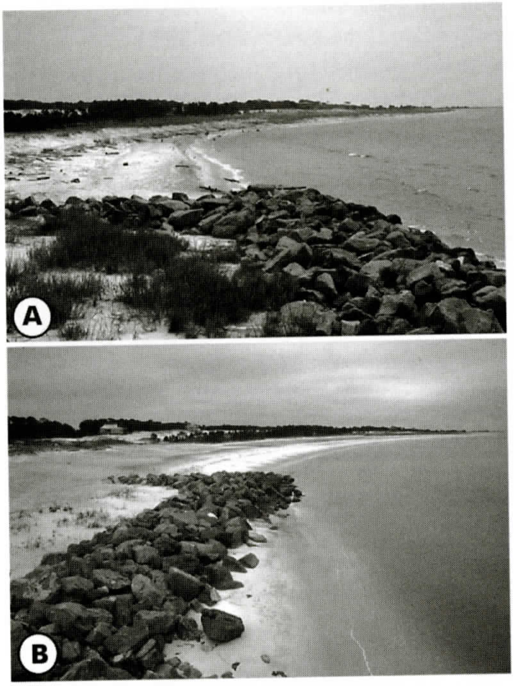

Figures 5A and 5B. Dauphin Island Pier area. Photograph (A) was taken August 1997, and photograph (B) was taken December 1998. In photograph 5A, the darkened area at the base of the berm crest is an outcrop of paleosol. Hurricane Georges storm surge and waves flattened the swash zone berm crest and washed landward to the base of the first large dune ridge. The paleosol outcrop was planed down and covered by sand washed shoreward during the course of the storm. This location is in Figure 1, Box B.

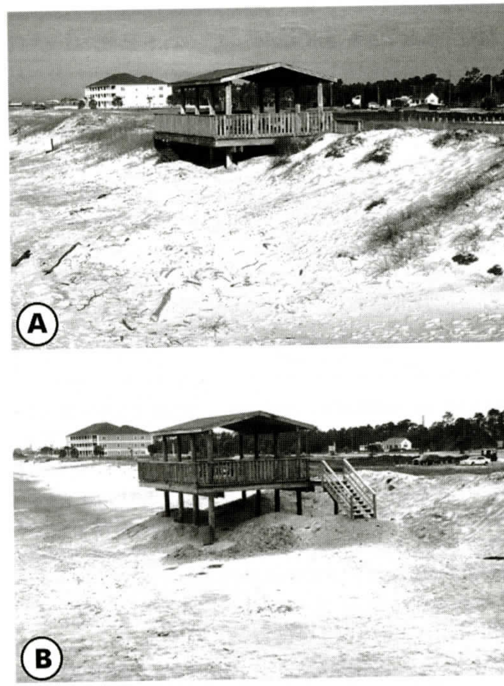

Figures 6A and 6B. Dauphin Island Picnic Area. Photograph (A) is from March 1998, and photograph (B) is from December 1998. This picnic pavilion (one of three) was constructed in the early 1980's on top of a series of large dune ridges adjacent to the beach. In subsequent years, the swash zone has moved shoreward and the backshore has been flattened to the point where this pavilion is in front of the last dune ridge. Note that sand was added around the base of the pavilion following Hurricane Georges in an attempt to protect it from further erosion and steps were constructed to allow continued access.

that extended along this portion of the beach (English and Haywick, 1996) was completely eroded flat and subsequently covered by quartz sand (Figures 5A and 5B). Vegetation that covered the nearshore portions of the backshore beach was removed during the storm.

Along the picnic area, Hurricane Georges's high water eroded and flattened a significant portion of the beach zone. Storm waves extended to the upland dune (Figures 6A and 6B). However, the addition of sand to the swash zone during the course of the storm resulted in little landward encroachment. The resulting beach profile dropped in elevation and was flattened and the gulf-facing side of the upland dune scarp was steepened.

Just west of the picnic area is an extensive section of beach where an exhumed soil containing the plant roots of a former pine (?) forest became exposed during Hurricane Danny in 1997. The organic material and associated exhumed soil were subsequently eroded away during Hurricane Georges and the entire beach profile was lowered in elevation, flattened, and broadened with accreted sand (Figures 7A and 7B).

The Western Developed And Undeveloped End Of Dauphin Island

The western portion of the island is an elon-

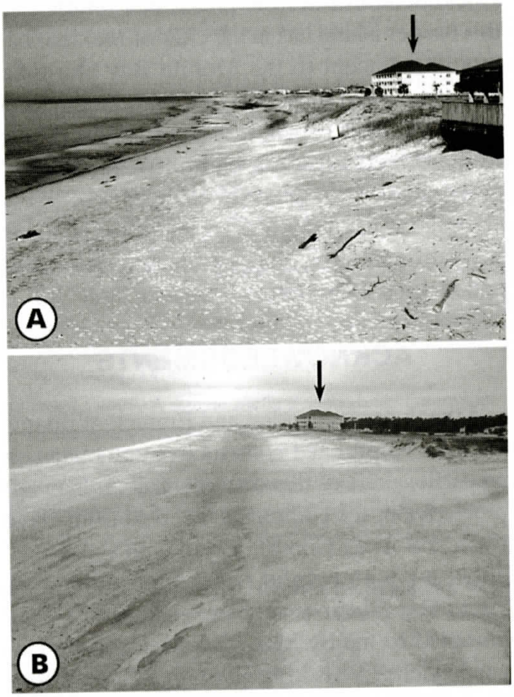

Figures 7A and 7B. Looking further west of the Dauphin Island Picnic Area. Photograph (A) was taken March 1998, and photograph (B) was taken December 1998. In 1997, Hurricane Danny eroded the backshore portion of this very narrow beach where an exhumed soil with pine (?) tree roots became exposed. This location is in the distance in the darkened area immediately shoreward from the large white building on the right. Hurricane Georges subsequently eroded away the area and washed sand shoreward. The result is a broadened and flattened beach. This location is in Figure 1, Box B.

Figures 8A and 8B. The residential western portion of Dauphin Island. Image (A) was taken July 1996, and image (B) was taken October 1998. Both images are facing north. Evident is the shortening of the beach and washover from the combination of storm surge and large storm waves. Both of these images are from the U.S. Geological Survey aerial pre- and post-Hurricane Georges assessment of the island. The photographs were obtained from the Internet and are used courtesy of the U.S. Geological Survey, Center for Coastal Geology. This location is in Figure 1, Box C.

gated narrow sand ridge with little relief (Nummedal and others, 1980; Smith and Parker, 1990; Smith, 1997). Hurricane Georges had sufficient storm surge energy and wave elevation to completely overwash much of this portion of Dauphin Island. The storm transported eroded swash zone and beach-derived sand northward across the thin slightly elevated ridge into the Mississippi Sound. This resulted in the further thinning of the island and the loss of some previously gulf-facing residential beach property (Figures 8A and 8B).

Further west along the same low-lying sand ridge in the undeveloped section of Dauphin Island, storm water was able to overwash much of this section of the island too (Figures 9A and 9B). Along this segment, the sand ridge can only develop as beach sand is blown ashore and held in place by vegetation. However, the short time intervals between storm events limits the natural development of this portion of the island and does little to prevent washover events from recurring.

DISCUSSION AND CONCLUSIONS

On September 28, 1998, Hurricane Georges impacted Dauphin Island as a Category 1 hurricane (*Saffir-Simpson* scale). A combination of

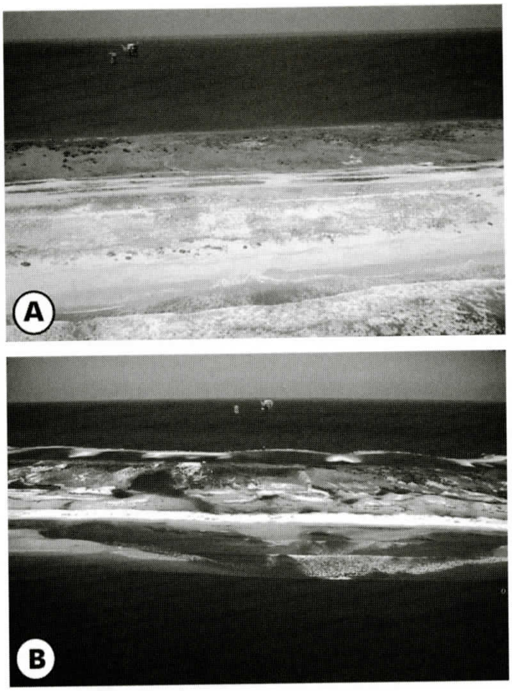

Figures 9A and 9B. Along the western end of the undeveloped portion of Dauphin Island. Photograph (A) was taken July 1996, and photograph (B) was taken October 1998. Both images are facing north. Before Hurricane Georges, there is extensive vegetation covering the back side of the sand ridge. Following the storm, almost all of the vegetation has been completely removed due to washover. The swash zone has moved landward by at least 10 meters and the transported sand now occurs as washover fan deposits in Mississippi Sound. Both of these images are from the U.S. Geological Survey aerial pre- and post-Hurricane Georges's assessment of the island. The photographs were obtained from the Internet and are used courtesy of the U.S. Geological Survey, Center for Coastal Geology. This location is approximated in Figure 1, Box D.

tidal surge and elevated storm waves penetrated well inland on the eastern end of the island and completely overwashed much of the western end. The gulf facing beach profile along the entire length of the island was transformed. Subsequent fair-weather conditions leading up to early 2005, have not returned the island to either its pre-Georges position or shape.

Hurricane Georges's impact across Dauphin Island demonstrates the precarious setting that this barrier island has in the Gulf of Mexico. Although adjacent to the Mobile Bay ebb-tidal delta the island must still rely on periodic sand nourishment. As such, it is extremely sensitive to the effects of storm and hurricane events. Storm-derived large-scale changes will likely continue as natural processes shape the island in ways different from the existing human-derived and maintained setting.

ACKNOWLEDGMENTS

I thank Jerry Akridge and Emmett Williams for their helpful and constructive comments on an earlier draft of this document. I am also appreciative of the comments received from Dave Bush and Andy Coburn. Ervin Otvos also provided me with helpful comments and discussion. Excellent reference assistance was provided to me by Mrs. Thajura Harmon. Eugene "Gene" Wilson, University of South Alabama Professor Emeritus, provided me with valuable information about Dauphin Island and I am grateful for his helpful assistance. Appreciation is expressed to the scientists of the U.S. Geological Survey, National Oceanic and Atmospheric Administration, National Aeronautics and Space Administration, and the National Weather Service for providing important and useful information about Hurricane Georges on the Internet. This work neither represents the views or opinions of the U.S. Environmental Protection Agency, nor was this investigation conducted in any official capacity.

REFERENCES CITED

Douglass, S.L., 1994, Beach erosion and deposition on Dauphin Island, Alabama, U.S.A.: Journal of Coastal Research 10:306-328.

Douglass, S.L., 2001, State of the beaches of Alabama, Accessed from: http://www.usouthal.edu/usa/cesrp/beaches2001.html

English, M. and Haywick, D.W., 1996, Stop 2: Exhumed soil profile at Dauphin Island Public Beach. *In* Hummell, R.L. and Haywick, D.W. eds. Coastal deposition and ecosystems of Alabama. Guidebook for the 33rd Annual Field Trip of the Alabama Geological Society.

Froede, C.R., Jr., 1998, Hurricane Danny precipitation-induced washout channels and their subsequent repair along the southeastern end of Dauphin Island, Alabama: Southeastern Geology 38(1):29-37.

Froede, C.R., Jr., 2005, A Hurricane Frederic generated storm-surge deposit exposed along a surf zone foredune scarp on Dauphin Island, Alabama: Journal of Coastal Research, In press.

Guiney, J.L., 1999, Preliminary report, Hurricane Georges, 15 September – 01 October 1998, National Hurricane Center. NOAA. Accessed from: http://www.nhc.noaa.gov/1998georges.html.

Hardin, J.D., Sapp, C.D., Emplaincourt, J.L., and Richter, K.E., 1976, Shoreline and bathymetric changes in the coastal area of Alabama: A remote sensing approach: Geological Survey of Alabama Information Series 50, Tuscaloosa, AL.

Liebens, J., 2000, A simple method to evaluate the impact of tropical cyclones on the coast: Hurricane Georges and the Gulf Coast: Shore and Beach 68(1):17-24.

NCDC-NOAA, 1999, Georges pummels Caribbean, Florida Keys, and U.S. Gulf Coast. National Climatic Data Center. Accessed from: http://lwf.ncdc.noaa.gov/oa/reports/georges/georges.html.

Nummedal, D., Penland, S., Gerdes, R., Schramm, W., Kahn, J., and Roberts, H., 1980, Geologic response to hurricane impact on low-profile Gulf Coast barriers: Transactions of the Gulf Coast Association of Geological Societies 30:183-195.

Penland, S., Nummedal, D., and Schramm, W.E., 1980, Hurricane impact at Dauphin Island, Alabama. *In* Edge, B.L., ed., Coastal Zone '80: Proceedings of the Second Symposium on Coastal and Ocean Management, American Society of Civil Engineers, Hollywood, Florida, p. 1425-1449.

Sanchez, T.A., and Douglass, S.L., 1994, Alabama shoreline change rates: 1970-1993. College of Engineering Report No. 94-1: University of South Alabama, Mobile, AL.

Schramm, W.W., Penland, S., Gerdes, R.G., and Nummedal, D., 1980, Effect of Hurricane Frederic on Dauphin Island, Alabama: Shore and Beach 48(3):20-25.

Smith, W.E., 1997, Geomorphology of coastal Mobile County, Alabama. Geological Survey of Alabama Bulletin 162: Environmental Geology Division, Geological Survey of Alabama. Tuscaloosa, AL.

Smith, W.E., and Parker, S.J., 1990, Profiles of Alabama Gulf beaches 1988-1989. Geological Survey of Alabama Information Series 68: Energy and Coastal Geology Division, Geological Survey of Alabama, Tuscaloosa, AL.

Stone, G.W., Wang, P., Pepper, D.A., Grymes, J.M., III., Roberts, H.H., Zhang, X., Hsu, S.A., and Huh, O.K., 1999, Studying the importance of hurricanes to the northern Gulf of Mexico coast: EOS v. 80, n. 27, p. 301 and p. 305.

Turnipseed, D.P., Giese, G.L., Pearman, J.L. Farris, G.S. Krohn, and Sallenger, A.H., Jr., 1998, Hurricane Georges: Headwater flooding, storm surge, beach erosion, and habitat destruction on the Central Gulf Coast. U.S. Geological Survey Water Resources Investigations Report 98-4231. Accessed from: http://ms.water.usgs.gov/ms_proj/reports/georges/.

U.S. Army Corps of Engineers, Mobile District. 1981. Hurricane Frederic post disaster report, 30 August - 14 September 1979. Mobile, AL.

U.S. Army Corps of Engineers, Mobile District. 1999. Hurricane Georges: Storm surge September 1998. Mobile, AL.

U.S. Geological Survey, 1982, Biloxi: MISS.-ALA.-LA., 1:100,000 scale topographic map.

U.S. Geological Survey, 2001, Hurricane Georges - Pre/post-storm oblique aerial photography: Center for Coastal Geology. Accessed from: http://coastal.er.usgs.gov/hurricanes/georges/.